UNIVERSIDADE D
COIMBRA

Beatriz Isabel Pelicano Cristóvão

LYSOSOMAL FUNCTION DURING *CANDIDA* INFECTION: CONNEXIN 43 AS A NEW PLAYER IN THE INFECTION PROCESS

Dissertação no âmbito do Mestrado em Investigação Biomédica, ramo de Infeção e Imunidade, orientada pela Doutora Neuza Luísa da Silva Domingues e pelo Doutor Henrique Manuel Paixão dos Santos Girão, apresentada à Faculdade de Medicina da Universidade de Coimbra.

Outubro de 2021

Faculdade de Medicina da Universidade de Coimbra

LYSOSOMAL FUNCTION DURING *CANDIDA* INFECTION: CONNEXIN 43 AS A NEW PLAYER IN THE INFECTION PROCESS

Beatriz Isabel Pelicano Cristóvão

Dissertação no âmbito do Mestrado em Investigação Biomédica, ramo de Infeção e Imunidade, orientada pela Doutora Neuza Luísa da Silva Domingues e pelo Doutor Henrique Manuel Paixão dos Santos Girão, apresentada à Faculdade de Medicina da Universidade de Coimbra

Outubro de 2021

Dissertação apresentada à Faculdade de Medicina da Universidade de Coimbra para cumprimento dos requisitos necessários à obtenção do grau de Mestre em Investigação Biomédica com especialização em Infeção e Imunidade. O trabalho apresentado foi realizado no Instituto de Investigação Clínica e Biomédica de Coimbra (iCBR) sob orientação científica da Doutora Neuza Luísa da Silva Domingues e pelo Doutor Henrique Manuel Paixão dos Santos Girão.

This work was financed by the European Regional Development Fund (ERDF), through the Operational Program for Competitiveness Factors (COMPETE; under the projects PAC “NETDIAMOND” POCI-01-0145-FEDER-016385; HealthyAging2020 CENTRO-01-0145-FEDER-000012-N2323; POCI-01-0145-FEDER-007440, CENTRO-01-0145- FEDER-032179, CENTRO-01-0145-FEDER-032414, POCI-01-0145-FEDER-022122; FCTUID/NEU/04539/2013, UID/NEU/04539/2019, UIDP/04539/2020; and FCT/PT2020-02/SAICT/2017_424 Repair

Agradecimentos

Em primeiro lugar, gostaria de agradecer a todos os que me acompanharam durante esta fase da minha vida!

À Neuza, minha amiga e estimada orientadora, em dose dupla, um agradecimento caloroso. Não esquecerei todos os ensinamentos e partilhas. Obrigada pela motivação diária, por todo o crescimento pessoal e científico e por toda a paciência que tiveste, especialmente, nesta última fase. Acima de tudo, muito obrigada por me transmitires todos os dias a tua grande paixão pela ciência!

Ao Professor Henrique, agradeço desde já por me ter aceite no g(u)ic e por todo o apoio e disponibilidade para comigo. Obrigada também por todas as excelentes discussões cientificas e por todo o conhecimento transmitido.

À Professora Teresa Gonçalves e à Lisa, agradeço por toda a cooperação e auxílio durante a realização deste projeto, também aos restantes membros do grupo MMYRG obrigada pela simpatia e boa disposição.

Ao meu vizinho de gabinete Jorge, um obrigada muito especial por toda a ajuda e por toda a paciência durante este último ano. Nunca esquecerei as inúmeras gargalhadas e momentos partilhados. À minha mais recente companheira de gabinete e de pausas para o lanche Luísa, obrigada por todas as palavras de carinho e motivação nos momentos certos.

A todos os g(u)ic o mais sincero obrigado, por todo o apoio demonstrado! À Zuza, à Carla, ao Steve, à Judy, à Mónica, à Teresa, à Dani, à Maria e à Tânia, agradeço toda a disponibilidade, ajuda e ensinamentos partilhados. À minha ex-companheira de gabinete Tatiana, obrigada pela companhia indispensável durante o último ano.

Aos meus amigos de Biologia, em especial à Diana, à Rita, à Jess e à Ruivinho, obrigada por estarem sempre lá para ouvir os meus desesperos e dramas. Agradeço também aos meus amigos de Coimbra que na companhia de um cafezinho, sempre estiveram disponíveis para os meus desabafos! À minha irmã de coração Maria, que mesmo estando longe, sempre me incentivou a sonhar mais além.

Ao Alexandre por teres estado lá quando eu mais precisava, por todo o carinho e conforto e, acima de tudo, por toda a paciência e compreensão, pois sei que não foi um ano fácil, um grande obrigada do fundo do coração!

Por último e mais importante à minha família: aos meus pais, ao meu mano e aos meus avós, um grande obrigada pelo apoio incondicional, força, paciência e por acreditarem em mim, desde sempre! «Avó, We did it!».

Table of contents

Figure Index

Table Index

Abbreviations

3-MA	3-Methyladenine
ALIX	ALG-2 interacting protein X
AMPK	AMP-activated protein kinase
ATG16L	Autophagy-related protein 16-1
ATG4B	Autophagy related 4B cysteine peptidase
Ca	*Candida albicans*
Ca^{2+}	Calcium
CBX	Carbenoxolone disodium salt
CC	Cellular component
CLEC7A	Dectin-1
CR3	Complement receptor 3
Cx43	Connexin 43
DEGs	Differentially expressed genes
EEA1	Early endosome antigen 1
ER	Endoplasmic reticulum
ERAD	Endoplasmic reticulum-associated degradation
ESCRT	Endosomal sorting complex required for transport
Gal3	Galectin 3
GJA1	Gap junction gene
H_2O_2	Hydrogen peroxide
HK	Heat-killed
IC	Invasive Candidiasis
ICAM3	Intercellular adhesion molecule 3
IL-18	Interleukin 18
IL-1β	Interleukin 1 beta
IP3	Inositol trisphosphate
ITGB2	β2-integrin
K^+	Potassium
LAMP	Lysosome-associated membrane protein
LAP	LC3-associated phagocytosis

LC3	Microtubule-associated proteins 1A/1B light chain 3B
LLOMe	L-leucyl-L-leucine O-methyl ester
LRRK2	Kinase leucine-rich repeat kinase 2
MCU	Mitochondrial Ca^{2+} uniporter
MINCLE	Macrophage-inducible C-type
mTORC1	Mammalian target of rapamycin complex 1
NADPH	Nicotinamide adenine dinucleotide phosphate
NLRP3	NLR family pyrin domain containing 3
O^-_2	Superoxide ions
PAMPs	Pathogen-associated molecular patterns
Panx1	Pannexin1
PBS	Phosphate-buffered saline
PRRs	Pattern recognition receptors
PVDF	Polyvinylidene difluoride
PXL	Paxillin
ROS	Reactive oxygen species
SEM	Standard error of the mean
SLRs	Sequestosome like receptors
SNAREs	Fusion-promoting soluble NSF attachment protein receptors
STRING	Search tool for the retrieval of interacting genes
TFEB	Transcription factor EB
TLN1	Talin
TLR4	Toll-like receptor 4
TNTs	Tunneling nanotubes
TRIM16	Tripartite motif-containing protein 16
Ub	Ubiquitin
ULK1	Serine/threonine-protein kinase ULK1
v-ATPase	Vacuolar H+-ATPase
VASP	Vasodilator-stimulated phosphoprotein
VCL	Vinculin

Resumo

Candidíase Invasiva (CI), uma infeção fúngica grave, pode ser causada por diversas espécies do género *Candida,* sendo *Candida albicans* a espécie mais predominante a nível mundial. *C. albicans* faz parte da flora da maior parte dos indivíduos saudáveis. Porém quando a imunidade do hospedeiro sofre perturbações, este fungo transita para um microrganismo oportunista. Os macrófagos fazem parte da primeira linha de defesa, tendo estas células a capacidade de internalizar e eliminar *C. albicans*, através da fagocitose. Após a internalização da *C. albicans,* o fungo sofre alterações na sua morfogénese, transitando para a forma de hifa, induzindo dano na membrana do fagossoma. Para garantir a sua sobrevivência, os macrófagos necessitam de uma resposta celular eficiente para combater rapidamente os danos celulares provocados pela hifa. Recentemente, a manutenção da integridade da membrana do fagossoma foi positivamente relacionada com o crescimento do tamanho da *C. albicans* e com a sua fuga. Foi também descrito um novo mecanismo de defesa envolvendo estruturas contráteis de actina em forma de anel, durante a infeção por *C. albicans*. Considerando estes estudos recentes, assim como a falta de conhecimento sobre os mecanismos moleculares envolvidos na reparação da membrana do fagossoma contendo a hifa, o nosso estudo teve como objetivo investigar os principais mecanismos responsáveis pela manutenção da integridade da membrana do fagossoma, utilizando uma linha de macrófagos RAW 264.7 infetados com *C. albicans*. Os nossos resultados sugeriram uma possível ativação da maquinaria de reparação, através do recrutamento da Alix e da Tsg101, ambas componentes da maquinaria de reparação *endosomal sorting complex required for transport* (*ESCRT),* para os fagossomas contendo *C. albicans*. Adicionalmente, observámos também o recrutamento de Trim16, um componente da maquinaria envolvida na lisofagia, para fagossomas contendo *C. albicans.* Os nossos resultados também indicaram que os mecanismos de biogénese lisossomal e de autofagia não fazem parte dos principais mecanismos de defesa envolvidos na resposta do macrófago à infeção por *C. albicans*. Adicionalmente demonstrámos que a capacidade do macrófago de dobrar hifas diminui com a perda da integridade da membrana do fagossoma e com a inibição da autofagia. Por último, para revelar novos intervenientes na resposta do macrófago à hifa em crescimento, realizámos também uma análise de dados publicados de transcriptómica de macrófagos infetados com *C. albicans*. Os nossos resultados demonstraram a conexina43 (Cx43) como um potencial *hit* durante a infeção por *C. albicans*. Efetivamente, foi observado um aumento do recrutamento da Cx43 para o fagossoma contendo *C. albicans*, assim como um aumento da capacidade dos

macrófagos de dobrar as hifas. Encontrámos também uma grande colocalização de Cx43 com as estruturas de actina que se encontravam ao redor do fagossoma contendo *C. albicans.* Em suma, o nosso trabalho revela novos dados sobre o impacto da integridade da membrana do fagossoma, da autofagia e da biogénese lisossomal, assim como um potencial papel novo não canónico da Cx43 na resposta imune do macrófago à infeção por *C. albicans*.

Palavras chave: *Candida albicans*, Integridade da membrana fagossomal, Autofagia, Dobra da hifa, Conexina 43

Abstract

Invasive Candidiasis (IC), a life-threatening fungal infection, can be caused by several *Candida* spp., being *Candida albicans* the most prevalent specie worldwide. *C. albicans* is a constituent of the microbiome in most healthy individuals. However, upon perturbations of host immunity, this fungus transits to an opportunistic pathogen. Macrophages are part of the first line of defense against infections as they can engulf and eliminate *C. albicans* through phagocytosis. After *C. albicans* engulfment, the yeast transits to a hyphal form inducing phagosomal membrane damage. In order to survive, macrophages require an efficient cellular response to rapidly counteract the hypha-induced cellular damage. Recently, the maintenance of the phagosomal membrane integrity was positively related with *C. albicans* length growth and escape. Furthermore, a new defense mechanism involving actin-contractile rings structures was elegantly described during *C. albicans* infection. Thus, considering these emerging studies and the lack of knowledge on the underlying molecular mechanisms involved in hypha-containing phagolysosomal membrane repair, we aimed to investigate the crucial mechanisms responsible to maintain phagolysosomal membrane integrity in macrophages infected with *C. albicans* by using a RAW 264.7 macrophage cell line. Our results suggested a potential activation of the repair machinery, through the recruitment of Alix and Tsg101, both components of the endosomal sorting complex required for transport (ESCRT) machinery, to *C. albicans* containing-phagosomes. In addition, we also observed a recruitment of Trim16, a lysophagy component, to the *C. albicans*-containing phagosome. Moreover, our results indicated that lysosomal biogenesis and autophagy were not the main defence mechanisms involved in macrophages response to *C. albicans* infection. Notably, we demonstrated that macrophage folding capacity decreased with loss of phagosomal membrane integrity and inhibition of autophagy. Lastly, to unveil new putative players involved in macrophages response to expanding hypha, we also performed an analysis of published transcriptomic data from *C. albicans* infected macrophages. Our findings highlighted Connexin43 (Cx43) as a potential hit during *C. albicans* infection. Indeed, we found that Cx43 is recruited to phagosomes containing *C. albicans* and potentiate the folding capacity of macrophages. We also observed a high colocalization of Cx43 with the actin ring structures surrounding the *C. albicans*-containing phagosome. Taken together, our data unveiled new insights on the impact of the phagosomal membrane integrity, autophagy and lysosomal biogenesis, as well as a new possible non-canonical role of Cx43 on the macrophage immune response to *C. albicans* infection.

Keywords: *Candida albicans*, Phagolysosomal membrane integrity, Autophagy, Hyphal folding, Connexin 43

Introduction

1. Introduction

1.1. Invasive Candidiasis

Candidiasis is a board term for cutaneous, mucosal and deep-seated organ infections caused by *Candida* genus fungi [1]. Invasive candidiasis (IC), one of the most common life-threatening fungal infections, involves candidemia, a bloodstream infection caused by *Candida* spp. and deep-seated infection, such as intra-abdominal abscess, peritonitis (inflammation of the peritoneum) or osteomyelitis (infection of the bones) **(Figure 1)**. IC has an estimated annual incidence of 750 thousand cases worldwide [2]. Moreover, IC is commonly found among hospitalized individuals, presenting a significant mortality and morbidity rates [3].

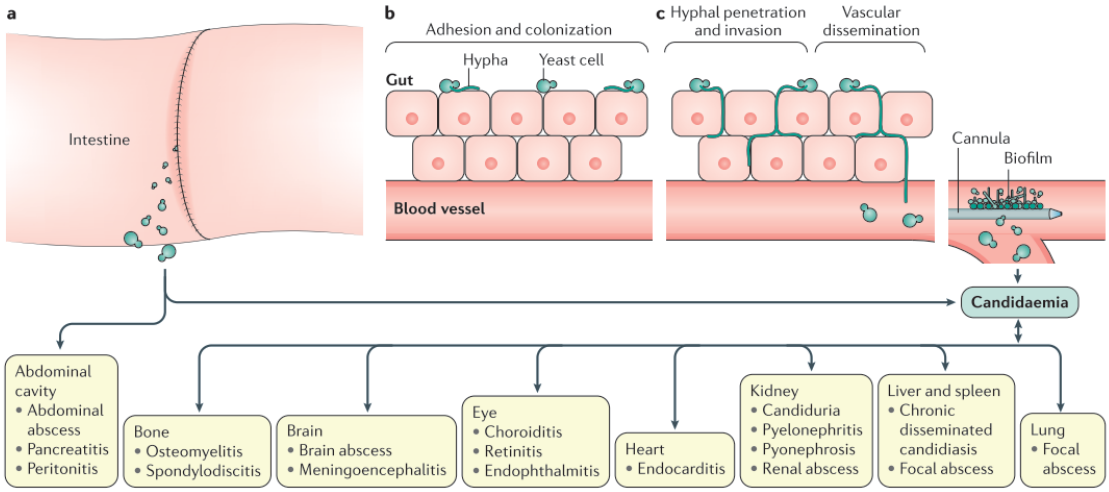

Figura 1 | Pathogenesis of Invasive Candidiasis
(A) *Candida* spp. are commensal organisms found in the gut microbiota. However, disruption of the gastrointestinal barriers, as after gastrointestinal perforation, *Candida* spp. can directly disseminate to the abdominal cavity and enter the bloodstream (Candidaemia). **(B)** Under normal conditions, the fungus behaves as a commensal organism without causing disease. **(C)** A deficient immune response can promote fungal overgrowth in the gut and candidaemia, which can lead to deep-seated opportunistic infections in various organs (Invasive Candidiasis). Adapted from [1].

Over the last decades, an increasing incidence of this fungal infection has been associated with a rise in the number of patients receiving hyperalimentation through catheters or probes and requiring organ transplantations as well as, the use of wide-spectrum antibiotics [4], [5]. Despite the extensive antifungal therapies and the improvements in the diagnosis and treatment [3], [6], increasing levels of resistance to antifungal drugs have been observed [6]. One of the main drivers of antimicrobial resistant are the misuse and overuse of antibiotics and immunocompromising drug

treatments [7]. Thus, it is urgent to design therapeutic strategies to overcome this health problem.

More than 95% of all invasive *Candida* infections are caused by 5 species: *Candida albicans*, *Candida glabrata*, *Candida parapsilosis*, *Candida tropicalis* and *Candida krusei* [8]–[10]. However, the distribution of the species abovementioned suffers variations depending on the geographical area [1], [10]. For example, *Candida auris*, a previously rare microorganism, has emerged as a major pathogen in the United States, Spain, the United Kingdom, Germany, Japan, Norway, among others [11]. In Europe and in the United States, *C. albicans* is the most prevalent specie responsible for invasive candidiasis **(Figure 2)** [12]. Concordantly, a more recent epidemiological study in the Eastern world demonstrated *C. albicans* as the most prevalent species causing IC [13].

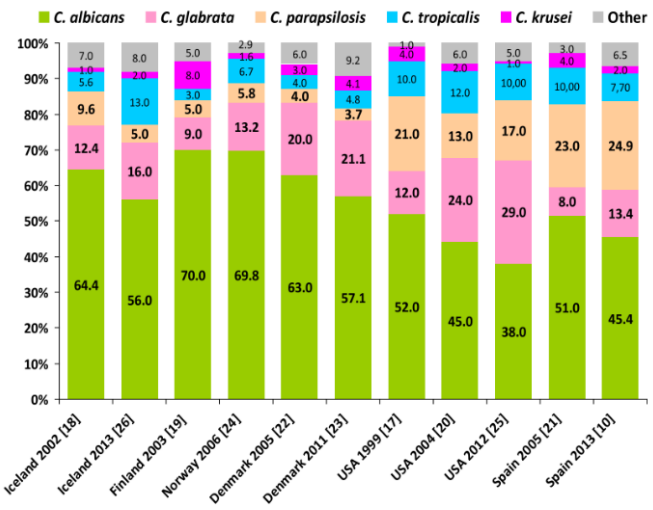

Figura 2 | Ranking of the top 5 *Candida* species is variable
Distribution of the most prevalent *Candida* species from population-based studies in different European countries and in the United States. Adapted from [2].

1.2. *Candida albicans*

C. albicans are commensal fungi present on the mucosal surfaces of several habitats of 50-70% of most healthy individuals [1]. Such microorganisms can live in the gut, throat, mouth and vagina, without causing any infection. Though, upon host environment alterations [14], this opportunistic pathogen may transit to a virulent and hostile phenotype generating mucosal infections. *C. albicans* can then escape from the host immune system and enter into the bloodstream and/or internal organs leading to

severe systemic infection, as candidemia, endocarditis and meningoencephalitis [1], [15]–[17].

C. albicans can appear in different morphological forms: yeast or blastospores, pseudohyphae and hyphae **(Figure 3)**. The unicellular yeast is an oval or spherical cell able to reproduce asexually by budding. Pseudohyphae and hyphae are morphologically different, since pseudohyphae have constrictions at the sites of septation and are thicker than hyphae. By contrast, hyphae form long tube-like filaments with no constrictions at the septa junctions [18], [19]. This polymorphism is a major factor of *C. albicans* pathogenicity [18]. Previous findings have demonstrated that *C. albicans* strains, locked in either the yeast or hyphal form, display diminished virulence [20], [21]. In addition, *C. albicans* yeast form is associated with commensal growth and bloodstream dissemination, whereas the hyphal form is related with tissue invasion [22], strengthening the importance of both forms and consequent phenotypic switch for its pathogenesis [23]. The yeast-to-hypha transition initiates due to multiple environmental stimuli, such as acidic pH, increased temperature, starvation and contact with the host immune system [24]. Consequently, each growing hypha presents its own membrane signature, due to the different environmental stimuli [18]. Furthermore, *C. albicans* has the ability to regulate immune cells morphology and metabolic pathways, as well as to stimulate its own survival within harsh host environments, including the macrophage phagosome [25]–[27].

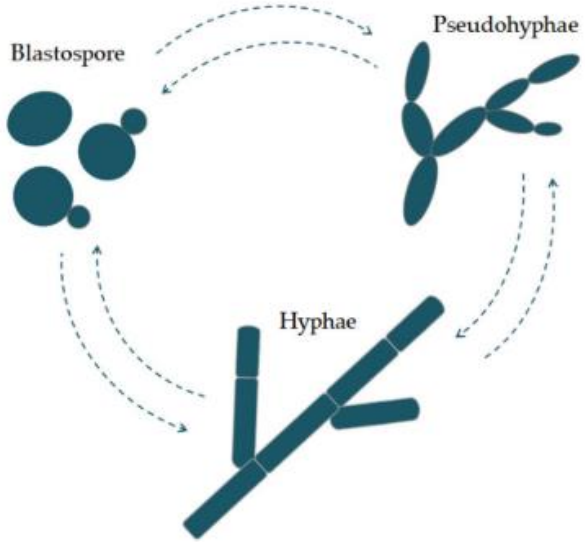

Figura 3 | *Candida albicans* morphology
The morphological transitions from blastospore, also known as yeast, to pseudohyphae and hyphae are reversible. Adapted from [19].

The major players in innate immunity that recognize invading pathogens and subsequently activate host response mediating fungal killing are macrophages and neutrophils. Neutrophils are short-lived and one of the first cell types to migrate to a site of inflammation. With a longer-lived, monocyte-derived macrophages are recruited to the infected tissue being responsible to engulf and eliminate the pathogens. Macrophages can directly control fungal proliferation and coordinate the response of other immune cells [27]. Experimental evidences demonstrated that upon depletion of mononuclear phagocytes fungal proliferation in tissues is accelerated, leading to an

increase in mortality [28], [29]. Nevertheless, although some *C. albicans* cells are effectively killed by macrophage engulfment, others can evade or survive macrophage interactions and persist in the host [30]. The outcome of this macrophage-*C. albican*s interaction remains unclear. Thus, here after, we will focus on the macrophage interaction with *C. albicans.*

1.3. Macrophage infection mechanism by *Candida albicans*

C. albicans cell wall, constituted by an inner layer and an outer layer, also known as matrix, is essential for the maintenance of the pathogen integrity and is also responsible for the fungus interaction with other cells and surfaces. The inner layer is mainly formed with β-glucan and chitin and the outer layer with glycosylated and mannoproteins [31], [32].

1.3.1. *Candida albicans* recognition

Macrophage recognition of *C. albicans* is mediated by the pathogen-associated molecular patterns (PAMPs) present at the fungal cell surface, which are recognized by the host macrophage pattern recognition receptors (PRRs) [33] **(Figure 4A)**. The major *C. albicans* PAMPs are: β-glucans which are recognized by dectin-1, a C-type lectin, and by complement receptor 3 (CR3) [33]–[36]; O-mannan which interacts with toll-like receptor 4 (TLR4); and N-mannan recognized by Dectin-2, dendritic cell-specific intercellular adhesion molecule 3 (ICAM3)-grabbing non-integrin (DC-SIGN) and macrophage-inducible C-type lectin (MINCLE) [33]–[35]. In addition, *C. albican*s phagocytic rate is dependent on the type of PRRs. Studies performed in J774.1A

macrophages demonstrated that upon Dectin-1 blockage the engulfment rate of *C. albicans* decreased [37]. Importantly, this phagocytic rate is also dependent of fungal morphogenesis, since macrophages exposed to *C. albicans* hyphal form presented a lower phagocytic rate [38], resulting in the formation of open tubular phagocytic structures [39]. Following *C. albicans* recognition, phagocytosis is initiated, encompassing phagosome formation and maturation.

1.3.2. Phagosome formation and maturation

Phagosome formation starts after PAMPs-PRRs binding, initiating the formation and extension of actin-dependent pseudopods around the yeast, until the phagosomal membrane is sealed [40]. This occurs with the transient increase of the phosphatidylinositol 4,5-*bis*phosphate ($PI(4,5)P_2$) levels, during the pseudopods extension [41]. Simultaneously, phospholipase Cγ is activated, leading to plasma membrane $PI(4,5)P_2$ hydrolysis and subsequent F-actin depolymerisation at the base of the phagocytic cup [40]. Moreover, $PI(4,5)P_2$ hydrolysis releases inositolphosphate-3 (IP_3), which mediates signalling events, such as the calcium (Ca^{2+}) release from the endoplasmic reticulum into the cytosol. This increased levels of cytosolic Ca^{2+} induces intracellular signalling cascades required for both phagosome formation and maturation [42]. Additionally, activation of the Dectin-1 receptor was showed to regulate the recruitment of microtubule-associated proteins 1A/1B light chain 3B (LC3) to the phagosomes containing *C. albicans* [43], promoting LC3-associated phagocytosis (LAP). Interestingly, inhibition of LC3 deconjugation was recently demonstrated to lead to LC3-associated phagosomes stabilization, through reactive oxygen species (ROS) production by nicotinamide adenine dinucleotide phosphate (NADPH) oxidase 2 (NOX2), in a process dependent on oxidative inactivation of autophagy related 4B cysteine peptidase (ATG4B) activity [44].

The nascent phagosome undergoes through a series of fusion and fission events initially involving the early endosomes and recycling endosomes [45], decreasing its pH (pH 6.1-6.5) [46]. These early events are regulated by GTPases, such as RAB5 and RAB7, early endosome antigen 1 (EEA1) and fusion-promoting soluble NSF attachment protein receptors (SNAREs) - Syntaxin 6 and Syntaxin 13 [47]–[50]. Later, early phagosomes fuse with late endosomes originating late phagosomes; which fuses with lysosomes forming phagolysosomes [51]. These fusion events deliver a large number of degradative enzymes, including proteases, lysozymes, and lipases [52], as

well as the NADPH oxidase responsible for ROS production [53]. The phagolysosomal acidification is progressively achieved through the proton-pumping vacuolar-type adenosine triphosphatase (V-ATPase) [54]. The highly acidic environment (pH 4.5-5.0) of this organelles, enables the optimal degradative capacity of lysosomal hydrolytic enzymes, contributing to pathogen clearance [55] **(Figure 4B)**.

Furthermore, during *C. albicans*-containing phagosomes maturation, the phagosome-lysosome fusion was demonstrated to be tyrosine-protein kinase SYK dependent [56]. This protein, which was previously demonstrated to play an fundamental role in complement-mediated phagocytosis [57], accelerates phagosome acidification by regulation of actin surrounding phagosomes and the subsequent fusion with lysosomes [36]. The authors also revealed that SYK depletion in macrophages permitted *C. albicans* survival due to insufficient phagosome acidification. Further studies have shown that knockdown of RAB14 hampers the recruitment of lysosome-associated membrane proteins 1 (Lamp1) to phagosomes containing *C. albicans* [58].

1.3.3. *Candida albicans* escape

Several studies have been describing the different strategies adopted by intracellular pathogens to survive and replicate inside host cells [59], however only a few studies have explored the intracellular fate of fungal pathogens [60]–[63]. Inside the mature phagosome, the high levels of microbicidal activities, such as the limited availability of nutrients, reactive molecular species, hydrolytic activities, and an acidic pH, *C. albicans* undergoes a significant metabolic change **(Figure 4C)**. Then, *C. albicans* can grow as hyphae within a few hours after phagocytosis **(Figure 4D)**. Though, hyphae were shown to facilitate escape by simple membrane piercing through mechanical force [64], [65], *C. albicans* escape was recently associated with the macrophage inflammasome-dependent cell death (pyroptosis) [66], [67]. Another mechanism used by hypha is the pore-forming toxin candidalysin, which induces direct membrane injury to the phagocytes [68]. A final escape mechanism resides on, non-lytic expulsion of *C. albicans* from macrophages, but this event seems to be less frequent [69]. Globally, hypha formation after phagocytosis is required for most of the described escape mechanisms.

1.4. Macrophage defence mechanisms

To counteract *C. albicans* infection, macrophages present several microbicidal activities. These activities are associated with an increase in ROS and reactive nitrogen species production, in acidic pH and hydrolytic environment, as well as a limited nutrient availability at the phagolysosome compartment. As mentioned earlier, ROS are produced in the phagolysosome lumen through the activation of NADPH oxidase [53], triggering the respiratory burst by producing superoxide ions (O_2^-) [70], and thereby converting it to hydrogen peroxide (H_2O_2) [71]. During this immunometabolic reprogramming, macrophages rapidly elevate cytosolic Ca^{2+} and consequently activate the mitochondrial Ca^{2+} uniporter (MCU), inducing an influx of Ca^{2+} into the mitochondria. This event leads to NADPH production and subsequent generation of phagosomal ROS. Interestingly, $MCU^{-/-}$ macrophages presented a deficient capacity to produce phagosomal ROS which impairs the elimination of phagocytosed *C. albicans* [72]. Another phagolysosomal strategy of macrophages to fight against *C. albicans* infection is through fungal cells intoxication with trace metals, such as copper. Since, upon *C. albicans* infection, copper accumulation on phagolysosomes favors the reaction with H_2O_2, originating a broader range of damaging ROS, through a process called Fenton reaction [73].

Acidic phagolysosomal pH also participates in antifungal macrophage strategies by conferring the ideal conditions for hydrolases activity (revised in detail by Flannagan, Cosío, & Grinstein, 2009). Originally, it was thought that acidic pH of the phagosomal lumen influenced the yeast-to-hypha transition [75]–[80]. *C. albicans* was suggested to manipulate the phagolysosomal pH by increasing the ammonia production, which would chelate phagolysosomal protons. This phagosomal lumen alkalinization was suggested to occur before hyphal transition, facilitating the morphological process [77]–[80]. Contradicting these findings, multiple evidences demonstrated an activation of the filamentation-associated and core filamentation genes after *C. albicans* engulfment [27]. Additionally, it was also demonstrated that yeast-to-hypha transition occurs inside the acidic vesicle and phagosomal alkalinization is acquired as consequence of the hyphal length growth, due to the stretch and eventual rupture of the phagosomal membrane [81].

A new defence mechanism of macrophages against *C. albicans* infection involving hyphae folding was demonstrated [82]. Through a actin-contractile ring, macrophages were able to constrict C. *albicans* hyphae, hamper their length growth, reduce macrophage escape, and facilitates their complete engulfment by the phagosome [82]

(Figure 4E). Thus, hyphal folding, joins the other antifungal strategies previously described, promoting successful fungal elimination.

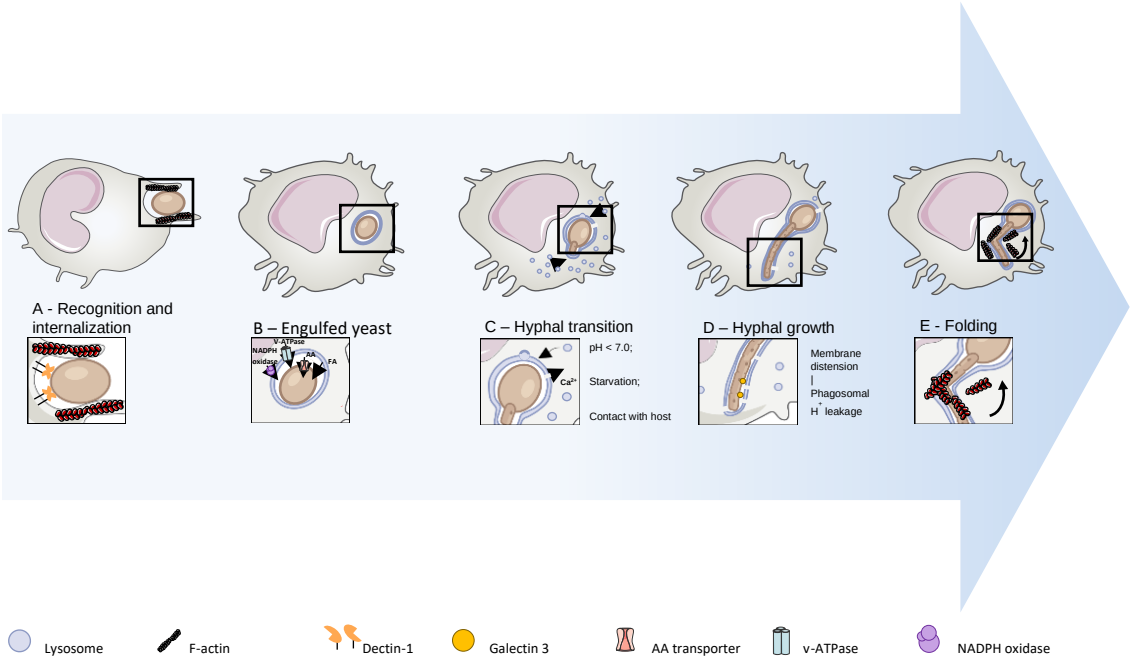

Figura 4 | A schematic overview of the intracellular life of *Candida albicans* inside macrophages
A. Recognition and internalization of *C. albicans*. Macrophages recognize the *C. albicans* pathogen-associated molecular patterns (PAMPs) via pattern recognition receptors (PRRs), such as dectin-1. Following PAMP-PRR binding, F-actin is polymerized leading to pseudopods extension around the yeast. **B. Engulfed yeast.** Upon entrance, *C. albicans* resides within the mature phagosome being exposed to a highly acidic pH, and reactive oxygen species (ROS) due to the presence of v-ATPases and nicotinamide adenine dinucleotide phosphate (NADPH) oxidases, respectively, as well as to a nutrient deprived environment. *C. albicans* upregulates pathways to acquire amino (AA) or fatty acids (FA) to overcome the lack of nutrients inside the phagosomal lumen. **C. Hyphal transition.** Simultaneously to increase the access host cell nutrients, *C. albicans* initiates the transition from the yeast the hyphal form, which is initiated as a response to phagosomal environmental perturbations, such as acidic pH, low nutrients and contact with the host receptors. To maintain its integrity, the phagosomes expand, through the insertion of lysosomes which is induced by the phagosomal calcium (Ca^{2+}) release. **D. Hyphal growth.** *C. albicans* hyphal extension can originate phagosomal membrane rupture, leading to protons (H^+) leakage. Upon rupture, *C. albicans* leads to the accumulation of Galectin-3 (Gal3) in the phagosomal membranes. **E. Hyphal folding.** F-actin forms contractile ring structures around the phagosomes containing the hyphae, which will induce hyphal folding, at the fungal septal junctions, subsequently damaging *C. albicans* integrity, impairing its length growth.

As aforementioned, *C. albicans* length growth can reach several µm per hour, which can induce damage on the phagosome membrane [81]. Nevertheless, the stretching capacity of lipid membranes is restricted (estimated to be only 3% of their resting area) [83], [84], which suggest that macrophages require an efficient repair capacity to maintain phagosomal membrane integrity and subsequently, cell survival. Considering the importance of these mechanisms to the present thesis, this topic will be better described at the section of “Lysosomal repair mechanism”.

Moreover, in condition of impaired phagosomal membrane, leakage of lytic enzymes from the phagosome in the cytosol promotes nod-like receptor pyrin domain containing 3 (NLRP3) inflammasome activation and subsequent exacerbated interleukin 1 beta (IL-1β) secretion, leading to macrophage death through pyroptosis [66], [85].

1.5. Lysosome as a crucial organelle involved in macrophage defence mechanism

Lysosomes are membrane-enclosed cytoplasmic organelles, with a highly acidic pH, being responsible for the degradation of several biological macromolecules, including proteins, lipids, carbohydrates and nucleic acids [86]. Functional lysosomes are crucial for an efficient host response to infection and to maintain a controlled inflammatory response. Lysosomes are produced when a vesicle from Golgi complex fuses with a vesicle derived from the plasma membrane named endosome after suffering a process of maturation. Endoplasmic reticulum (ER) synthesizes the lysosomal enzymes and delivers it to lysosomes via specific pathways [87]. The lysosomal transmembrane proteins are heavily glycosylated on their luminal side forming a barrier that protects against autodigestion, named glycocalyx [88]. The most predominant are the lysosome-associated membrane protein (LAMP)1 and 2 (LAMP)2, combining about 80% of total lysosomal membrane proteins [88].

Lysosomes were considered the cell garbage disposal system. However, this point of view has been changed by recent discoveries. Lysosomes were also been involved in several other cellular processes besides degradation, such as gene regulation, immunity, metabolic signalling and cell migration, adhesion, apoptosis, plasma membrane repair, formation of invasive protrusions in cancer cells and secretion of lysosomal cargo, as observed in the bone resorption [86], [89]. Thus, in order to survive, cells need to ensure the normal function of this organelle.

1.5.1. Lysosomal damage

Lysosomal membrane rupture can induce cell apoptosis. Therefore, maintenance of its integrity is vital for cellular homeostasis [90]. As aforementioned, pathogens, such as *C. albicans,* are able to physically rupture the lysosomal membrane. Injured lysosomes leak their content to the cytosol leading to the activation of several cellular pathways. In

the next sections, we will describe the known mechanism involved in cellular response to damaged lysosomes, highlighting the ones associated with *C. albicans* infection.

1.5.2. Lysosomal repair mechanism

Upon membrane disruption the phagosome contents, such as secreted proteins from the fungal cells, ROS and host proteases, are released to the cytosol, inducing an increase in the cytosol acidity and damaging several cellular components [91]. In order to circumvent detrimental cellular event, cells activate an endolysosomal damage response (thoroughly reviewed by Papadopoulos, Kravic, & Meyer, 2020 and by Papadopoulos & Meyer, 2017). This response is initiated by the repair of moderate lysosomal membrane rupture, with a rapid recruitment of the endosomal sorting complex required for transport (ESCRT) machinery [93] **(Figure 5)**. Previously, by treating cells with lysosomotropic compounds [94], [95], ESCRT machinery components were demonstrated to be recruited to the injured sites.

The ESCRT machinery is organized into four distinct subcomplexes, ESCRT-0, ESCRT-I, ESCRT-II and ESCRT-III [96]–[98], of which the latter is thought to mediate membrane sealing/scission through formation of membrane-active oligomeric filaments [99], [100]. ESCRT recruitment to the ruptured membrane is triggered through the lysosomal Ca^{2+} release, which activates the lipid-binding activity of ALG-2 interacting protein X (Alix), an ESCRT-III component [101]. The recruitment of these components is also dependent of Tsg101, an ESCRT-I component [99]. Additionally, a recent study has demonstrated that Galectin 3 (Gal3) recruits Alix to the damaged lysosomes, being also required for the lysosomal restoration function [102].

Several phagolysosomal membrane repair mechanisms are already described to be involved in cellular response upon bacterial infection. In *Mycobacterium tuberculosis* infection, specific effectors of this pathogen were found to impair phagosomal maturation and antagonize the ESCRT machinery recruitment to the ruptured sites, thus inhibiting the repair and/or removal of injured phagolysosomes [103]. In *C. albicans* infection the recruitment of the repair machinery was only observed in macrophages containing yeast [104]. Kinase leucine-rich repeat kinase 2 (LRRK2) was shown to promote the recruitment of the Rab GTPase, Rab8A, to damaged endolysosomes as well as the ESCRT-III component CHMP4B, thereby inducing ESCRT-mediated repair [104], [105]. In epithelial cells infected with *C. albicans*, damaged membrane regions from the phagosome were eliminated through an Alg-

2/ALIX/ESCRT-III-dependent blebbing process and a repair of plasmalemmal vesicles induced *via* exocytic insertion of lysosomal membranes [106]. Moreover, previous work from the same group, showed that phagosomal expansion mechanism to escort the growth of *C. albicans* hyphae is a process dependent of Ca^{2+}-mediated lysosome fusion [85].

Although the limited data regarding the role of repair mechanism in expanding hypha-containing phagolysosomes, the reported mechanism may be a common defence strategy in host-pathogen interactions. As consequence of an efficient repair of limited membrane rupture, lysosomes can be reacidified and later refilled with cathepsins [107].

1.5.3. Lysophagy mechanism

Upon failure of the ESCRT machinery repair, cells initiate the removal of damaged lysosome through a type of selective autophagy, namely lysophagy [90]. Lysophagy is triggered by the recruitment of cytoplasmic proteins such as galectins, e.g. Gal3 **(Figure 5)**. This protein is a sensitive marker for lysosomal damage, through the recognition of exposed intraluminal carbohydrate chains of lysosomal glycoproteins from damaged lysosomes [95]. Gal3 interacts with the tripartite motif 16 protein (TRIM16), an E3 ubiquitin ligase. Then, proteins of the lysosomal membrane are ubiquitinated and autophagic machinery is recruited, as Serine/threonine-protein kinase ULK1 (ULK1), Autophagy-related protein 16-1 (ATG16L) and Beclin-1 [99], [108]. E2 ubiquitin-conjugating enzyme UBE2QL1 is a key ligase in this process, providing a large proportion of damage-induced ubiquitination responsible for the recruitment of ATG16L complex and autophagy receptors including SQSTM1/p62 [109]. Ultimately, ATG16L complex is responsible for the activation of LC3B and, together with the ULK1 complex, initiates the formation of the phagophore. [90].

The role of lysophagy was never addressed during *C. albicans* infection. However, recent work showed that upon inhibition of lysosomal fusion with the expanding hypha-containing phagosome, Gal3 was recruited to the membrane of this organelle. Due to the dual role of Gal3 on the recruitment of ESCRT and lysophagic components [102], further studies are needed to investigate whether lysophagy can play a role during the macrophage response to the growing hypha.

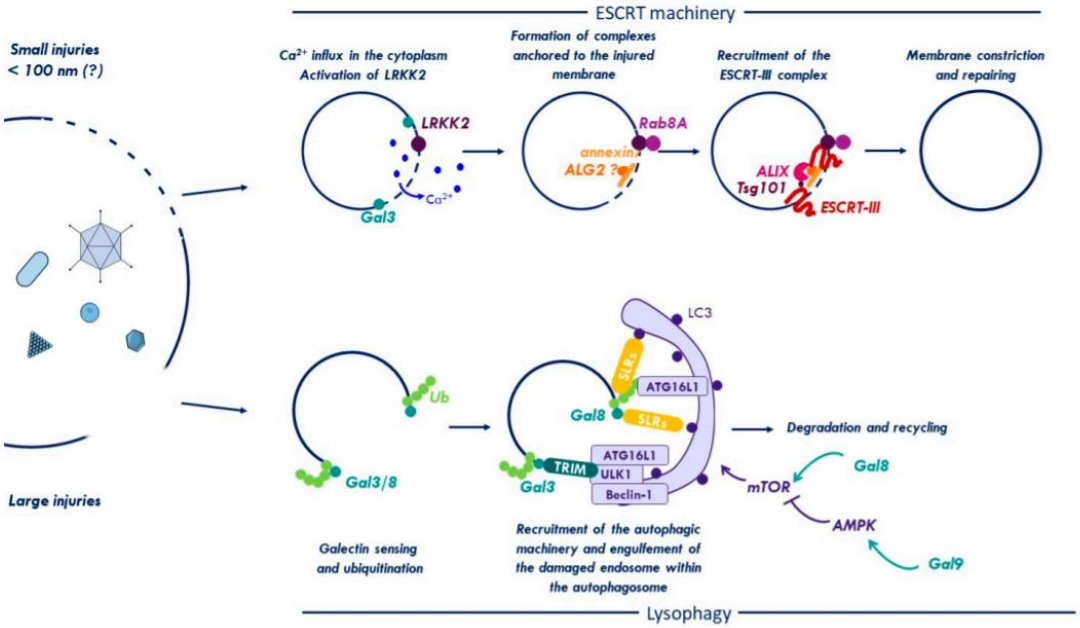

Figura 5 | Repair and removal of damaged lysosomes
Small injuries in the lysosomal membrane trigger calcium (Ca^{2+}) leakage into the cytosol and activate LRKK2, which promotes the recruitment of the small GTPase Rab8A. The cytosolic annexin7 and the calcium sensor ALG2 are also recruited to the injured site. Subsequently, two endosomal sorting complexes required for transport (ESCRT) components, ALIX and Tsg101, are recruited to the membrane damage site promoting membrane repair by the endosomal sorting complexes required for transport (ESCRT) machinery. Galectin-3 (Gal3) is recruited to damage sites and may promote ESCRT assembly. Larger damage or inefficient repair lead to lysophagy. Damaged lysosomes are sensed and tagged by galectins, such as Gal3, and ubiquitin. Then, the recruitment of proteins of the autophagic machinery are recruited, such as Serine/threonine-protein kinase ULK1 (ULK1), Autophagy-related protein 16-1 (ATG16L) and Beclin-1, are mediated by autophagic receptores, such as the sequestosome like receptors (SLRs) or tripartite motif proteins TRIMs. The residues of the damaged membrane are engulfed in a double-membrane vesicle called autophagosome, which fuses with lysosomes for content degradation and recycling. Autophagy is also controlled by metabolic kinase mechanistic target of rapamycin (mTOR) through Gal8. Moreover, activation of the AMP-activated protein kinase (AMPK) is mediated by Gal9 in response to membrane damage to inhibit mTOR. Adapted from [108].

1.5.4. Lysosomal biogenesis

The biogenesis of lysosomes involves the maturation of various endocytic vesicles as, early endosomes and late endosome. The identification of a transcriptional gene network required in multiple aspects of lysosomal function and autophagy named “CLEAR” – coordinated lysosomal expression and regulation – was essential in the understanding of this lysosomal process [110]. Additionally, *de novo* synthesis of lysosomes is managed by transcription factor EB (TFEB), which is translocated from the cytosol to the nucleus, to become activated [91]. Moreover, TFEB localization is defined by its phosphorylation state. The TFEB recruitment to the nucleus can be initiated by dephosphorylation via calcineurin, a Ca^{2+}/calmodulin dependent phosphatase [111]. During cellular response to damaged lysosomes, galectin 8 were showed to inhibit mammalian target of rapamycin complex 1 (mTORC1) activity [86].

This mTORC1 inhibition activates the translocation of TFEB from the cytosol to the nucleus, thus inducing the expression of genes associated with lysosomal biogenesis and autophagy, enabling damaged lysosome to be recycled and/or replaced [102], [112].

As briefly mentioned, an internal source of membrane derived from lysosomes was showed to be responsible to maintain the membrane integrity of phagosomes containing expanding hyphae of Candida albicans [85]. Upon *C. albicans* recognition and engulfment., the authors also reported a nuclear redistribution of TFEB as a compensatory mechanism to restore the lysosomal pool [85]. Notably, this TFEB activation was in a calcineurin-independent manner [85].

1.6. Connexin: an "omnipresent" protein

In general, infection by pathogens causes cellular damage which activates a complex inflammatory response. Typically, this response leads to the release of proinflammatory cytokines, chemokines and free radicals that were found to modulate the activity of the gap junctions and hemichannels [113]–[115].

Connexins (Cxs) are transmembrane proteins associated with intercellular communication, being expressed in almost all cell types, tissues and organs [116]. These proteins consist of four α-helical transmembrane domains and two extracellular loops that are highly conserved among several connexins, an intracellular loop and a N- and C- terminal domains [117]. The assemble of six connexin subunits generates hexameric structures named connexin hemichannels, also known as connexons [118]. Connexin hemichannels are transported to the plasma membrane, where they dock with opposing hemichannels of neighbour cells to form gap junction channels, allowing the communication between the intracellular and the extracellular environment, releasing paracrine or autocrine signaling molecules [119]. Furthermore, beyond its channel function at the plasma membrane, connexins can generate small fragments and isoforms, that are normally present in diverse cellular compartments such as the nucleus, where they could have an alternative function as regulation of gene transcription or cell growth [120]. Connexins are considered a dynamic family of proteins, due to their short half-life, 1-2.5 hours, from synthesis to degradation [121]. Thus, modulation of the turnover rate of connexins is a crucial mechanism upon gap junctions regulation [122].

Connexin43 (Cx43) is the most widely expressed Cx [123], being encoded by the GJA1 gene and associated with direct cell to cell communication through gap junctions **(Figure 6)**. As earlier mentioned, the half-life of Cx43 is short and its degradation is dependent on the proteasome and autophagy activity, and the lysosome pathway [124]. Interestingly, the endoplasmic reticulum-associated degradation (ERAD), a protein quality control process that degrades irregular proteins in the proteosome, is responsible for the degradation of 40% of Cx43 [122]. The remain Cx43 is degraded in the lysosome, reaching this organelle through the endocytic pathway or macroautophagy [125]. Our group have shown that Cx43 degradation through macroautophagy requires Nedd4-mediated ubiquitination and subsequent interaction with the endocytic adaptor Eps15 and the autophagy adaptor p62, mediating the recognition of ubiquitinated substrates [126].

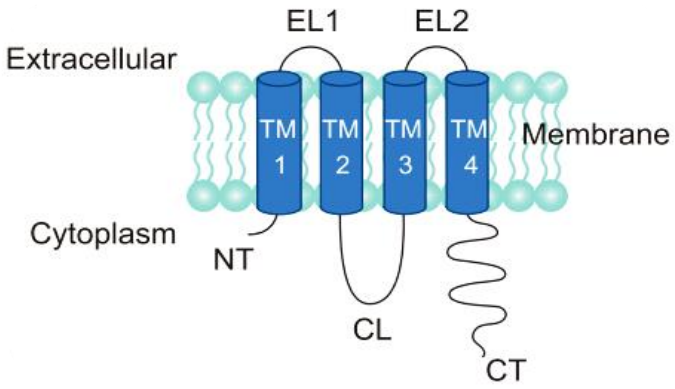

Figura 6 | A schematic representation of Cx43 structure
Cx43 transmembrane protein contains four α-helical transmembrane domains (TM1–TM4), two extracellular loops (EL1 and EL2), a cytoplasmic loop (CL) between TM2 and TM3, and cytoplasmic N-terminal (NT) and C-terminal (CT) domains. Adapted from [119].

1.6.1. Connexin43 canonical roles – intercellular communication

Classical intercellular communication is mediated by hemichannels of adjacent cells which generate gap junction plaques [127]. These plaques allow the direct exchange of several molecules, as microRNAs, second messengers, small metabolites, ions, and peptides. Thus, the gap junction mediated intercellular communication is crucial for the coordination of cell and organ function, as well as, for the preservation of the homeostasis [119].

1.6.2. Connexin43 non canonical roles – inflammation

Behind its role in direct intercellular communication, Cx43 has also been associated with several non-canonical roles, such as modulation of cell differentiation, adhesion, proliferation, as well as gene transcription, mitochondrial homeostasis, autophagy regulation, intracellular trafficking and in the stimulation and modulation of the immune responses [116], [119], [127]–[129]. However, these non-canonical functions are still poorly understood.

Previously, it was showed that Cx43 knockdown increased the number of differentiated neurons and impaired glial cell differentiation [130]. In mitochondria, Cx43 was also reported to modulate ROS production, potassium (K^+) influx to the matrix, ATP levels and respiration. Moreover, genetic deletion or transient knockdown of Cx43 affects gene expression implicated in cell adhesion and migration, as well as cytoskeleton dynamics and cell signalling, proliferation and differentiation processes [reviewed in [116]].

An alternative mechanism of extracellular vesicles–cell interaction was also ascribed to Cx43 [127]. Hexameric Cx43 structures were found at the extracellular vesicles surface, facilitating the rapid release of intraluminal contents directly into the cytoplasm of target cells [127]. In addition, a second mechanism of communication between nonadjacent cells is through actin-based cytoplasmic extensions comprising open-ended channels called tunneling nanotubes (TNTs) [131]. The presence of Cx43 in TNTs was associated with channel-mediated transfer of ions, small metabolites, or second messengers, such as $Ca^{2+}$and inositol trisphosphate (IP3) [119].

1.6.2.1. Connexin43 role during macrophage immune response

Previously, Cx43 was found to be upregulated in macrophages during sterile injurious as well as infectious inflammatory diseases, such as ischemia/reperfusion injury and sepsis [132]. Additional studies have also demonstrated that Cx43 upregulation decelerated wound healing [133]. Moreover, downregulation of Cx43 was reported to be decrease atherosclerosis progression, due to a reduced macrophage-induced chemotaxis and subsequent accumulation [134]. Notably, the opening of these hemichannels was showed to be regulated by inflammatory stimulus, secreting cytokine [135], [136]. However, further investigation is required to unveil the role of Cx43 in other macrophages functions, such as phagocytosis and polarisation.

Objectives

2. Objectives

The main goal of this thesis is to determine the mechanisms responsible to maintain the integrity of the phagolysosomal membrane during *C. albicans* infection. In order to achieve this, the following objectives were proposed:

1. Investigate the impact of lysosomal membrane integrity, autophagy and lysosomal biogenesis during *C. albicans* infection.
2. Evaluate -*C. albicans*' hypha folding as a new macrophage response upon *C. albicans* infection.
3. Assess the recruitment of Cx43 to damaged phagolysosomes containing the filamentous *C. albicans*, as well as the effect of Cx43 modulation during the infection process.

Materials and Methods

3. Materials and Methods

3.1. Chemicals

L-leucyl-L-leucine methyl ester (LLOMe) (L7393), carbenoxolone disodium salt (CBX) (C4790-1G) and 3-Methyladenine (3-MA) (M9281-500MG), were purchased from Sigma-Aldrich/Merck. 1,2-Bis(2-aminophenoxy)ethane-N,N,N′,N′-tetraacetic acid tetrakis(acetoxymethyl ester) (BAPTA-AM) was obtained from Calbiochem (196419).

3.2. Strain and Growth conditions

Candida albicans SC5314 was obtained from the Microbiology Pathogenic Yeast Collection, University of Coimbra.

Yeasts cells were grown at 30 °C overnight in YPD (0.5 % yeast extract, 1 % peptone, 2 % agar, and 2 % glucose) agar plates, harvested by centrifugation, and resuspended in phosphate-buffered saline (PBS) (pH 7.4). Yeasts were heat-killed (HK) at 95 °C, during 30 min. The fungal cells were counted in a Neubauer chamber and adjusted to the required cell density.

3.3. Cell culture

Experiments were carried out using the RAW 264.7 macrophage cell line, obtained from the European Collection of Cell Cultures (ECACC 91062702). RAW 264.7 cells were cultured and maintained in Dulbecco's Modified Eagle Medium (DMEM; Life Technologies, Carlsbad, CA, USA), supplemented with 10 % non-inactivated fetal bovine serum (FBS; Gibco, Life Technologies), 3.7 g/L sodium bicarbonate (Thermo Fisher Scientific), 1 % Penicillin/Streptomycin (Pen/Strep 100 U/mL:100 µg/mL; Life Technologies) at 37 ºC, in a humidified atmosphere with 5 % CO_2.

3.4. *Candida albicans* infection assays

RAW cells ($1.05x10^5$ cell/cm^2) were seeded in 6- or 24-well plates and allowed to adhere and stabilize for 24 h at 37 ºC, in a humidified atmosphere with 5 % CO_2. Macrophages were then washed with PBS and infected with *C. albicans* (multiplicity of infection [MOI], 1:1), for 1 h at 37 ºC (pulse), in a humidified atmosphere with 5 % of

CO_2. Then the non-adherent yeast cells were washed and *C. albicans* were allowed to internalize for 30 min or 180 min (chase). Cells were treated with 3-MA (20 μM) and CBX (10 μM) 60 and 10 min prior to infection, respectively, and compounds were maintained during the experiment time. BAPTA-AM (20 μM) was added at the chase time. LLOMe (500 μM) was added 10 and 30 min before the end of the infection period, 30 and 180 min, respectively. Incubation time points were 30 min, characterized for a higher number of *C. albicans* in the yeast form, and 180 min characterized for an increasing number of *C. albicans* in the hyphal form.

3.5. Cell infection with the lentiviral vector

RAW cells were incubated with the lentiviral vector pLenti6-CMV-V5-Cx43 and 8 μg/mL of polybrene for 20 min at room temperature. Then, cells were centrifuged for 90 min at 800× g and 32 °C, plated and incubated with 8 μg/mL of blasticidin. Overexpression of Cx43 in RAW cell line was investigated by western blot and immunofluorescence analysis. In order to isolate single cell clones from the polyclonal pool, limiting dilution cloning (LDC) in 96-well plate was applied by targeting 0.5 cells/well in complete growth medium, then transferring 100 μL of this to each. Plates were then incubated at 37 °C, 5 % CO_2 incubator. and the clonal expansion was monitored during the next days. Overexpression of Cx43 on the monoclonal RAW cell lines was confirmed by western blot and immunofluorescence analysis.

3.6. Immunofluorescence and image acquisition

After each timepoint (30 or 180 min after infection), the glass coverslips were fixed with 4 % paraformaldehyde (pH 7.4) in PBS for 15 min at room temperature. Then the samples were washed, followed by quenching of the aldehyde groups with ammonium chloride (concentration 50 mM) in 1 % PBS for 12 min and afterwards blocked with a solution of 0.05 % (w/v) saponin and 1 % (w/v) BSA, in PBS (blocking solution), for 30 min prior to incubation with primary antibodies overnight at 4 ºC in a humidified chamber (antibody list in Table 1). The coverslips were then washed with PBS and incubated with the secondary antibody for 1 h at room temperature, in a humid chamber. After this, they were washed with PBS and mounted with MOWIOL 4-88 Reagent (Calbiochem, San Diego, CA, USA). Nuclei were stained with 4’,6-diamidino-2-phenylindole dihydrochloride (DAPI) (Sigma-Aldrich). The images were collected by

fluorescence microscopy using a Zeiss Axio HXP IRE 2 microscope (Carl Zeiss AG) or by confocal microscopy using a Zeiss LSM 710 (Carl Zeiss AG), using ×63 oil immersion objective. Images were then analysed and quantified using Image J (detailed described in the section of “Phagocytic assay”, “Measurement of the percent of phagosomal proteins” and “Measurement of Lamp-1 intensity”) and Imaris softwares. Surface rendering was performed in 8- to 15-µm z-stack images composed of 0.43-µm optical slices using Imaris software (Bitplane AG, Switzerland) and carried out at the Imaging facility at iCBR (iLab - FMUC).

3.7. Immunoblotting

At the end of each timepoint (30 or 180 min, post-infection), RAW cells were detached and centrifugated at 1200 rpm, for 5 min, at 4 ºC. Then, the supernatants were removed, and cell pellets were washed with PBS and again centrifugated at 1200 rpm, for 5 min, at 4 ºC. Cell pellets were lysed to obtain total protein extracts using 2x Laemmli buffer [20 % (v/v) glycerol, 10 % (v/v) ß-mercaptoethanol, 4 % (v/v) SDS, 0.006 % (w/v) bromophenol blue and 125 mM Tris, pH 6.8]. The cell lysates were then sonicated in a Vibra Cell Sonicator, heated at for 5 min at 95 ºC and loaded on 10-15 % SDS polyacrylamide gels, using Precision Plus Protein™ Dual Color Standards (BioRad) or GRS Protein Marker MultiColour (GRiSP Research Solutions) as protein ladders. After electrophoresis, proteins were electrotransferred for 2 h at 300 mA with gentle agitation into polyvinylidene difluoride (PVDF) membranes, which were previously activated in methanol. To control protein loading, PVDF membranes were stained with Ponceau S. After washing, membranes were blocked with 1 % BSA or 5 % of milk (w/v) in TBS-T for 30 min at room temperature and then incubated, overnight at 4 ºC, with the primary antibodies diluted in blocking solution. Then, the membranes were washed three times with TBS-T for 10 min and incubated with the respective horseradish peroxidase (HRP)-conjugated secondary antibodies diluted in blocking solution, for 1 h at room temperature. The antibodies used are listed in Table 1. Lastly, the proteins were visualized by chemiluminescence with Clarity Western ECL substrate (Bio-Rad) using ImageQuant LAS 500 (GE Healthcare). The images were quantified using Image Lab 6.0.1 software from BioRad.

Table 1 | List of antibodies for immunofluorescence and immunoblotting analysis

Antibody	Host/Clonality	Clone/Cat#	Application	Dilution	Company
anti-*Candida albicans*	rabbit	GTX40096	IF	1:600	Genetex
anti-LAMP1	rat	1D4B	IF/WB	1:200/1:1000	DHSB (Developmental Studies Hybridoma Bank)
anti-Alix	mouse	SC - 53540	IF/WB	1:100	Santa Cruz
anti-Tsg101	mouse	AB83	IF/WB	1:100/1:1000	Abcam
anti-Galectin3	mouse	SC - 32790	IF/WB	1:100/1:1000	Santa Cruz
anti-LC3	rabbit	PA1 - 16930	WB	1:500	Thermo Fisher Scientific
anti-p62	rabbit	#51145	WB	1:500	Cell Signalling
anti-Beclin1	rabbit	A - 00023	WB	1:500	Sigma
anti-Cx43	goat	AB0016 – 500	IF/WB	1:200/1:1000	SICGEN
anti-goat HRP	rabbit	61-1620	WB	1:5000	Life Technologies
anti-mouse HRP	goat	626520#	WB	1:5000	BioRad
anti-rabbit HRP	goat	656120#	WB	1:5000	BioRad
anti-rat HRP	goat	62-9520	WB	1:5000	Invitrogen
anti-goat Alexa Fluor 488	donkey	A11055	IF	1:500	Invitrogen
anti-rabbit Alexa Fluor 488	goat	A-11008	IF	1:500	Invitrogen
anti-mouse	donkey	A10 037	IF	1:500	Invitrogen

Alexa Fluor 568					
anti-rat Alexa Fluor 594	donkey	A21209	IF	1:500	Invitrogen
anti-mouse Alexa Fluor 647	donkey	A31571	IF	1:500	Invitrogen
anti-rabbit Alexa Fluor 647	donkey	A31573	IF	1:500	Invitrogen

3.8. Phagocytic assay

Phagocytosis was performed with Aldehyde/Sulfate latex beads, 4 % w/v, 3.9 µm diameter (Thermo Fisher Scientific). IgG-opsonized beads were washed three times with PBS and opsonized in 20 % of rabbit serum for 60 min at room temperature under gentle rotation. For the phagocytosis assay a pulse-chase experiment was performed: the pulse time was 30 and 180 min. Non internalized beads were visualized with Alexa Fluor 647-conjugated donkey anti-rabbit antibody. The phagocytic index was calculated as (nº of cells with Beads/Total Beads) x (% of beads per cell) and quantified using the ‘‘Cell Counter’’ plugin from ImageJ software.

3.9. Measurement of the percent of phagosomal proteins

Percent of the proteins in the phagosomal membrane was estimated by measuring the intensity of phagosome-associated protein per the total cellular intensity of the specific protein x 100 at different time points (30 min and 180 min post-infection) using ImageJ software. For protein detection, a threshold was applied. Each phagosome was manually designing using the boundaries of *C. albicans* and/or Lamp-1 staining.

3.10. Measurement of Lamp-1 intensity

To quantify the total intensity of cellular Lamp-1, cells were manually outlined. The Lamp-1 objects were automatically identified using “Analyse Particles” function from ImageJ software after background removal and application of a threshold.

3.11. Gene set enrichment analysis

The RNA expression profiling of GSE111731 dataset was used in this study. The differentially expressed genes (DEGs) were obtained by the application of a linear model to the voom transformed data, using the limma package, for the statistical programming language R. Heatmaps were generated with Complex heatmap package for the statistical programming environment R. This analysis was carried out by a team member, Mónica Abreu, PhD. The DEGs involved in all the pathways related with vesicles and cell migration GO cellular component (CC) terms were intersect, resulting in 47 common genes. The search tool for the retrieval of interacting genes (STRING) database (11.5) was applied to integrate known and predicted protein-protein interactions for all these **(Figure 7)**. We also assessed their interaction with the molecular players already described to have a pivotal role in *C. albicans* hyphal constriction mechanism, namely: Dectin-1 (CLEC7A), β2-integrin (ITGB2) and vasodilator-stimulated phosphoprotein (VASP), from the recent work showing their involvement in hyphal folding and damage [82]; and talin (TLN1), paxillin (PXL), and vinculin (VCL), SYK, Formin (*FMN1* gene), HS1 (*HCLS1* gene), PYK2 (*PTK2B* gene) and FAK (*PTK2* gene), all proteins presented in actin cuff [39]. The correlation between these proteins was evaluated and displayed.

Figura 7 | Macrophages infected with *Candida albicans* present differentially expressed genes (DEGs) commonly associated to vesicles and cell migration
Venn diagram demonstrates the intersection of all the DEGs shared between vesicular trafficking and cell migration related GO: cellular components.

3.12. Statistical analysis

All data were analysed using GraphPad Prism Software (Version 6.01). The legends of the figures describe the exact number of independent experiences that were analyzed in each experiment. Results were presented as mean ± standard error of the mean (SEM). Statistical significance was determined using one-way ANOVA and two-way ANOVA followed by Dunnett's or Tukey's multiple comparison test, respectively, with a $p < 0.05$, considered statistically significant.

Results

4. Results

4.1. ESCRT machinery is recruited to hypha-containing phagosome

Professional phagocytes, such as macrophages, play a crucial role in *C. albicans* elimination from the host [33]. However, the exact defence mechanisms adopted by these cells to restrain the expanding hypha inside the phagosome remains to be clarified. To unveil the mechanism behind the phagolysosomal homeostasis during hyphal growth, we started by addressing the involvement of phagosomal membrane integrity, lysophagy and lysosomal biogenesis, in the macrophage's response upon *C. albicans* infection **(Figure 8A)**. For this, we investigated the recruitment of specific key proteins to the phagosome. Firstly, considering the importance of ESCRT machinery during the membrane repair of injured lysosomes [95], we evaluated the recruitment of two ESCRT components, Alix and Tsg101, to the phagosome containing *C. albicans*. RAW cells were infected with *C. albicans* and then immunostained for Alix, Tsg101 and Lamp-1, which identifies late endosomes and lysosomes. Our results revealed an increase in the recruitment of Alix to phagolysosomes containing *C. albicans*, after the yeast transitioned to the hyphal form **(Figure 8B)**. However, in the presence BAPTA-AM, a cytosolic Ca^{2+} chelator, this recruitment was reduced. BAPTA-AM was previously demonstrated to inhibit the Ca^{2+}-dependent recruitment of ESCRT machinery [95] and lysosomal insertion into *C. albicans*-containing phagosomes [85]. In addition, when infected macrophages were treated with LLOMe, which induces lysosome rupture, a more extensive colocalization of Alix with Lamp1 staining was observed. To further investigate the importance of this protein in the membrane of the expanding phagosome, we assessed the fraction of cellular Alix recruited to the phagolysosomes containing the growing hypha **(Figure 8C)**. Our data demonstrated that the length of the internalized *C. albicans* positively correlates with the increase of the phagosomal Alix fraction, thus suggesting that hyphal elongation promotes Alix recruitment to the phagosome. Nevertheless, expression levels of Alix during the infection time of macrophages were not significantly affected **(Figure 8D and 8E)**. Similar results were obtained when macrophages were infected with heat-killed (HK) *C. albicans* or when phagolysosomal rupture was induced by LLOMe treatment. Additionally, our immunofluorescence images showed an increase in the recruitment of Tsg101, to hypha-containing phagolysosomes **(Figure 8F)**, without significant alteration in total protein levels **(Figure 8G and 8H)**. Overall, these results indicate that ESCRT components are recruited to phagosomes containing *C. albicans*, suggesting an activation of the repair machinery upon yeast-to-hypha transition.

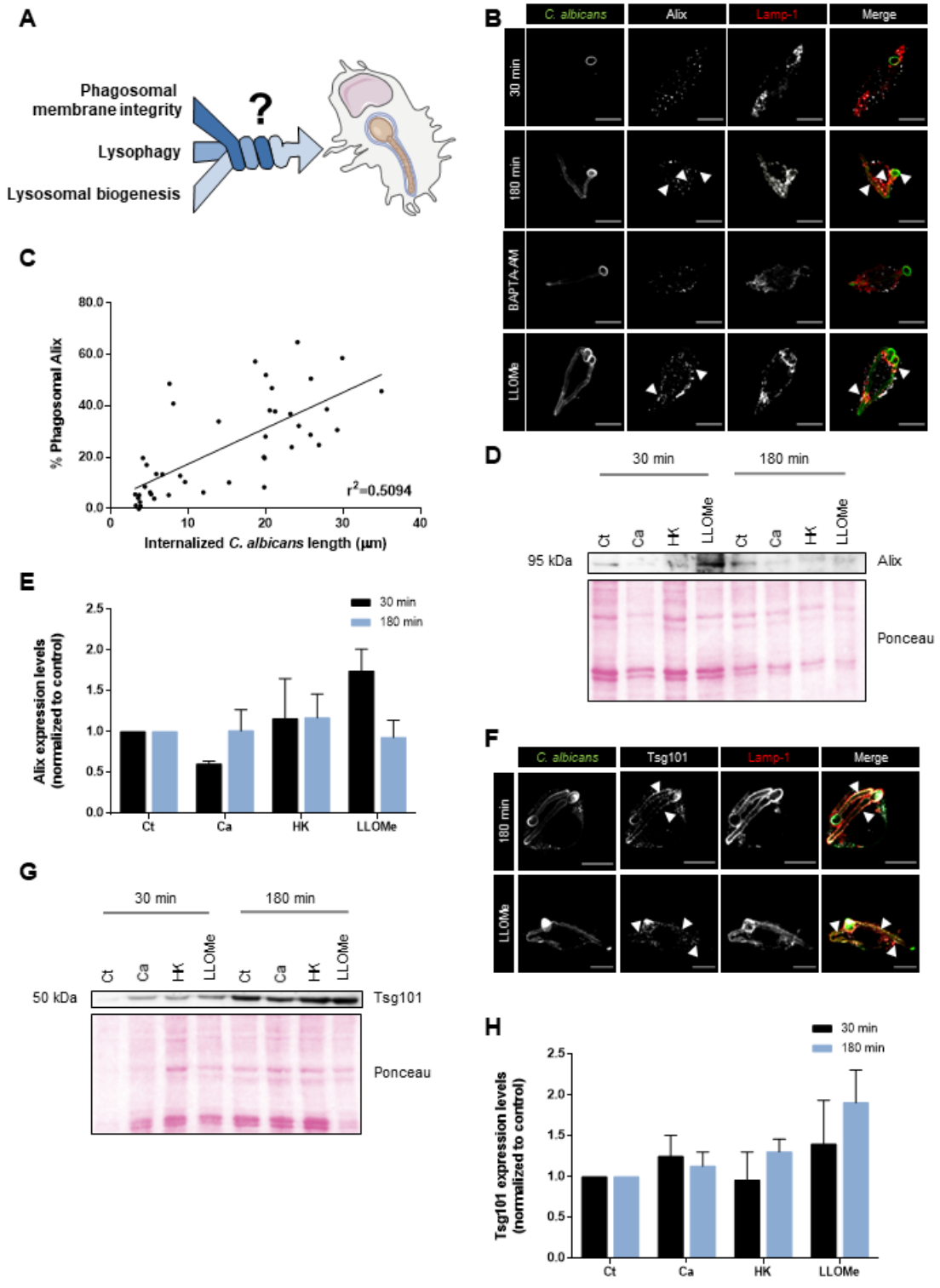
A
Phagosomal membrane integrity
Lysophagy
Lysosomal biogenesis
?
B
C. albicans
Alix
Lamp-1
Merge
30 min
180 min
BAPTA-AM
LLOMe
C
% Phagosomal Alix
Internalized C. albicans length (µm)
r²=0.5094
D
30 min
180 min
Ct
Ca
HK
LLOMe
95 kDa
Alix
Ponceau
E
Alix expression levels (normalized to control)
30 min
180 min
F
C. albicans
Tsg101
Lamp-1
Merge
G
50 kDa
Tsg101
H
Tsg101 expression levels (normalized to control)

Figura 8 | Internalized *Candida albicans* recruits ESCRT components to the expanding phagosomal membrane
(A) Schematic representation of the proposed pathways involved in the cellular response to the stressed phagosomes induced by hyphal growth. **(B)** Representative confocal images of RAW cells infected with *C. albicans*, fixed after 30 or 180 min post-infection, and immunostained for *C. albicans*, Alix and Lamp-1. Macrophages infected during 180 min were also treated with BAPTA-AM or LLOMe, to inhibit Alix recruitment or induce lysosomal injury (positive control), respectively. Scale bar, 10 µm. White arrowheads indicate sites of Alix accumulation around phagosome containing hypha. **(C)** Linear regression analysis correlating the length of internalized *C. albicans* and percentage of phagosomal Alix quantified as (phagosomal Alix/total Alix)*100, in RAW cells. Results were obtained from 3 independent experiments. At least 10 cells were analysed per experiment. **(D)** Representative immunoblot image and **(E)** quantification of Alix protein total levels upon RAW cells infection with *C. albicans* (Ca) or heat-killed (HK) *C. albicans*, or incubated with LLOMe, for 30 or 180 min. Results represent the mean ± SEM from 3 independent experiments. Ponceau was used as loading control. **(F)** Representative confocal images of RAW cells infected with *C. albicans,* fixed after 180 min post-infection, and immunostained for *C. albicans*, Tsg101 and Lamp-1. Scale bar, 10 µm. White arrowheads indicate sites of Tsg101 accumulation around the phagosome containing hypha. **(G)** Representative immunoblot image and **(H)** quantification of Tsg101 protein total levels upon RAW cells infection with Ca or HK, or incubated with LLOMe, for 30 or 180 min post-infection. Results represent the mean ± SEM from 4 independent experiments. Ponceau was used as loading control.

4.2. Hyphal growth induces recruitment of lysophagy components

Deficient repair of damaged lysosomes by the ESCRT machinery leads to the digestion of these vesicles through a process of selective autophagy, named lysophagy [91]. This process involves the recruitment of proteins, such as Gal3, Trim16, a Gal3 effector, and Ubiquitin [137]. Thus, we proposed to investigate the recruitment of these proteins to the phagosome containing *C. albicans*. Gal3 immunofluorescence imaging **(Figure 9A)** showed a slightly increase in Gal3 recruitment to the phagolysosome upon hypha formation. This finding was associated with only a moderate positive correlation between the fraction of cellular Gal3 with the expanding phagosome **(Figure 9B)**. In fact, macrophages infected with *C. albicans* and treated with LLOMe, presented a higher recruitment of Gal3 to Lamp1 positive vesicles, without a significant increase in the hypha-containing phagosome. Moreover, an increase in Gal3 expression levels was observed at 30 min post-infection, when compared with control cells, followed by an accentuated decrease of protein expression levels, at 180 min post-infection **(Figure 9C and 9D)**. Macrophages infected with HK or treated with LLOMe also presented diminished levels of Gal3 expression after 180 min of incubation. Furthermore, immunofluorescence detection of Trim16 **(Figure 9E)** showed that upon hyphal elongation, the distribution of Trim16 around the hypha-containing phagolysosomes was increased, when compared with the yeast form. Interestingly, similar with Gal3 results, LLOMe did not induce an increase in Trim16 recruitment to hypha-containing phagosome, but it substantially increased the recruitment to other Lamp1 positive vesicles. We also assessed the cellular fraction of Trim16 recruited to

the hypha-containing phagolysosomes **(Figure 9F)**. Interestingly, the obtained results demonstrated a stronger positive correlation between the length of the internalized *C. albicans* with the levels of Trim16 around the phagolysosome than those of Gal3. These results were not reflected by changes in the total levels of Trim16 **(Figure 9G and 9H)**. Similar to Gal3, our data also showed a slight recruitment of ubiquitin to the hyphae-containing phagosomes **(Figure 9I)**, with only a small correlation of the hyphae length with the phagosomal ubiquitin fraction **(Figure 9J)**. Altogether, these observations suggest that lysophagy components, mainly Trim16, are recruited to the phagolysosome as a response to the phagolysosomal rupture induced by hyphal growth.

4.3. Host defence against *Candida albicans* does not activate autophagy

Considering the crucial role of autophagy in the removal of damaged organelles, we speculated whether *C. albicans* infection could impact the autophagic capacity of macrophages. Activation of autophagy was measured by assessing the expression levels of autophagic components, including Beclin1, p62 and LC3. Our results demonstrated that, upon *C. albicans* infection, there was no significant effect in the total expression levels of Beclin1 **(Figure 10A and 10B)**. Similar results were obtained when p62 protein total levels were analysed, showing no statistical differences between infected macrophages and control cells **(Figure 10C and 10D)**. In macrophages infected with HK or treated with LLOMe, Beclin1 and p62 presented similar expression levels as control cells, with the exception of HK-infected macrophages that presented decreased levels at 30 min. During the autophagic process LC3 is lipidated into LC3-II, and incorporated into autophagosome membrane, *functioning as an autophagolysosomal marker*. Our results showed no significant changes in LC3-I and LC3-II expression levels in live *C. albicans* and HK infected macrophages **(Figure 10E to 10G)**, with no differences in the ratio LC3-II/LC3-I when compared to control cells **(Figure 10H)**. As expected, LLOMe treated macrophages presented a decrease in LC3-I levels and an increase in LC3-II, revealing an increased LC3-II/LC3-1 ratio, at 180 min post-infection. The transition of yeast to hypha was previously associated with an increased in TFEB translocation to the nucleus of infected macrophages, suggesting a stimulation of *de novo* synthesis of lysosomes [85]. To address whether lysosomal biogenesis could be a pivotal defence strategy of macrophages upon *C. albicans* infection, we next investigated Lamp1 expression levels during infection.

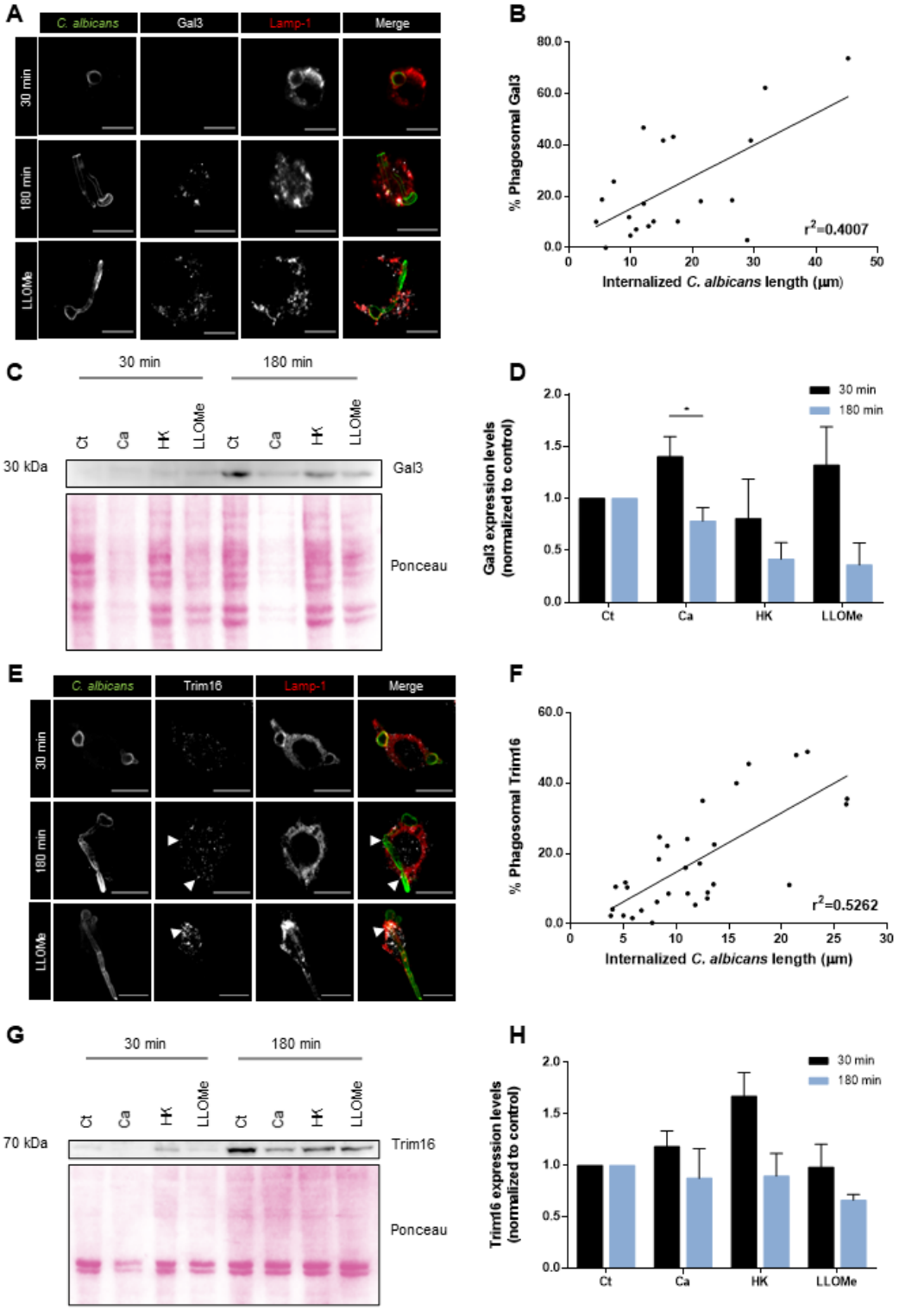
A
C. albicans
Gal3
Lamp-1
Merge
30 min
180 min
LLOMe
B
% Phagosomal Gal3
Internalized C. albicans length (µm)
r²=0.4007
C
30 min
180 min
Ct
Ca
HK
LLOMe
30 kDa
Gal3
Ponceau
D
Gal3 expression levels (normalized to control)
30 min
180 min
E
C. albicans
Trim16
Lamp-1
Merge
F
% Phagosomal Trim16
Internalized C. albicans length (µm)
r²=0.5262
G
70 kDa
Trim16
Ponceau
H
Trim16 expression levels (normalized to control)

Continuation of figure 2

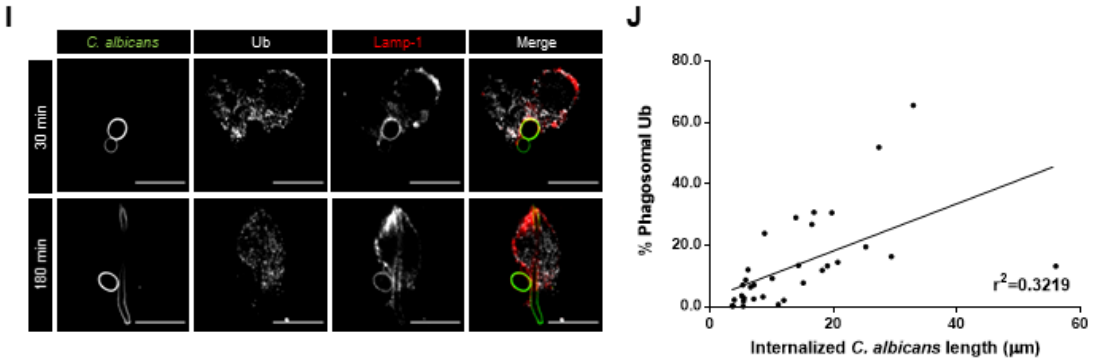

Figura 9 | Expanding phagosomes present Trim16, a component of lysophagy machinery, but not Galectin3 or ubiquitin

(A) Representative confocal images of RAW cells infected with *C. albicans*, fixed after 30 or 180 min post-infection, and immunostained for *C. albicans*, Galectin3 (Gal3) and Lamp-1. Macrophages infected for 180 min were also treated with LLOMe to induce lysosomal injury (positive control). Scale bar, 10 µm. White arrowheads indicate sites of Gal3 accumulation around the phagosome containing hypha. **(B)** Linear regression analysis correlating the length of internalized *C. albicans* and percentage of phagosomal Gal3 quantified as (phagosomal Gal3/total Gal3)*100, in RAW cells. Results were obtained from 3 independent experiments. At least 5 cells were analysed per experiment. **(C)** Representative immunoblot image and **(D)** quantification of Gal3 protein total levels upon RAW cells infection with Ca or HK, or incubated with 500µM of LLOMe, for 30 or 180 min. Results represent the mean ± SEM from 7 independent experiments. *p*-values were calculated by a one-way ANOVA followed by Dunnett's multiple comparisons test ($*p < 0.05$), compared to Ca 30 min. Ponceau was used as loading control. **(E)** Representative confocal images of RAW cells infected with *C. albicans*, fixed after 30 or 180 min post-infection, and immunostained for *C. albicans*, Trim16 and Lamp-1. Macrophages infected during 180 min were also treated with LLOMe. Scale bar, 10 µm. White arrowheads indicate sites of Trim16 accumulation around the phagosome containing hypha. **(F)** Linear regression analysis correlating the length of internalized *C. albicans* and percentage of phagosomal Trim16 quantified as (phagosomal Trim16/total Trim16)*100, in RAW cells. Results were obtained from 3 independent experiments. At least 5 cells were analysed per experiment. **(G)** Representative immunoblot image and **(H)** quantification of Trim16 protein total levels upon RAW cells infection with *C. albicans* (Ca) or heat-killed (HK) *C. albicans,* or incubated with 500µM of LLOMe, for 30 or 180 min. Results represent the mean ± SEM from 3 independent experiments. Ponceau was used as loading control. **(I)** Representative confocal images of RAW cells infected with *C. albicans*, fixed after 30 or 180 min post-infection, and immunostained for *C. albicans*, Ubiquitin (Ub) and Lamp-1. Scale bar, 10 µm. White arrowheads indicate sites of Ub accumulation around phagosome containing hypha. **(J)** Linear regression analysis correlating the length of internalized *C. albicans* and percentage of phagosomal Ub quantified as (phagosomal Ub/total Ub)*100, in RAW cells. Results were obtained from 1 independent experiment

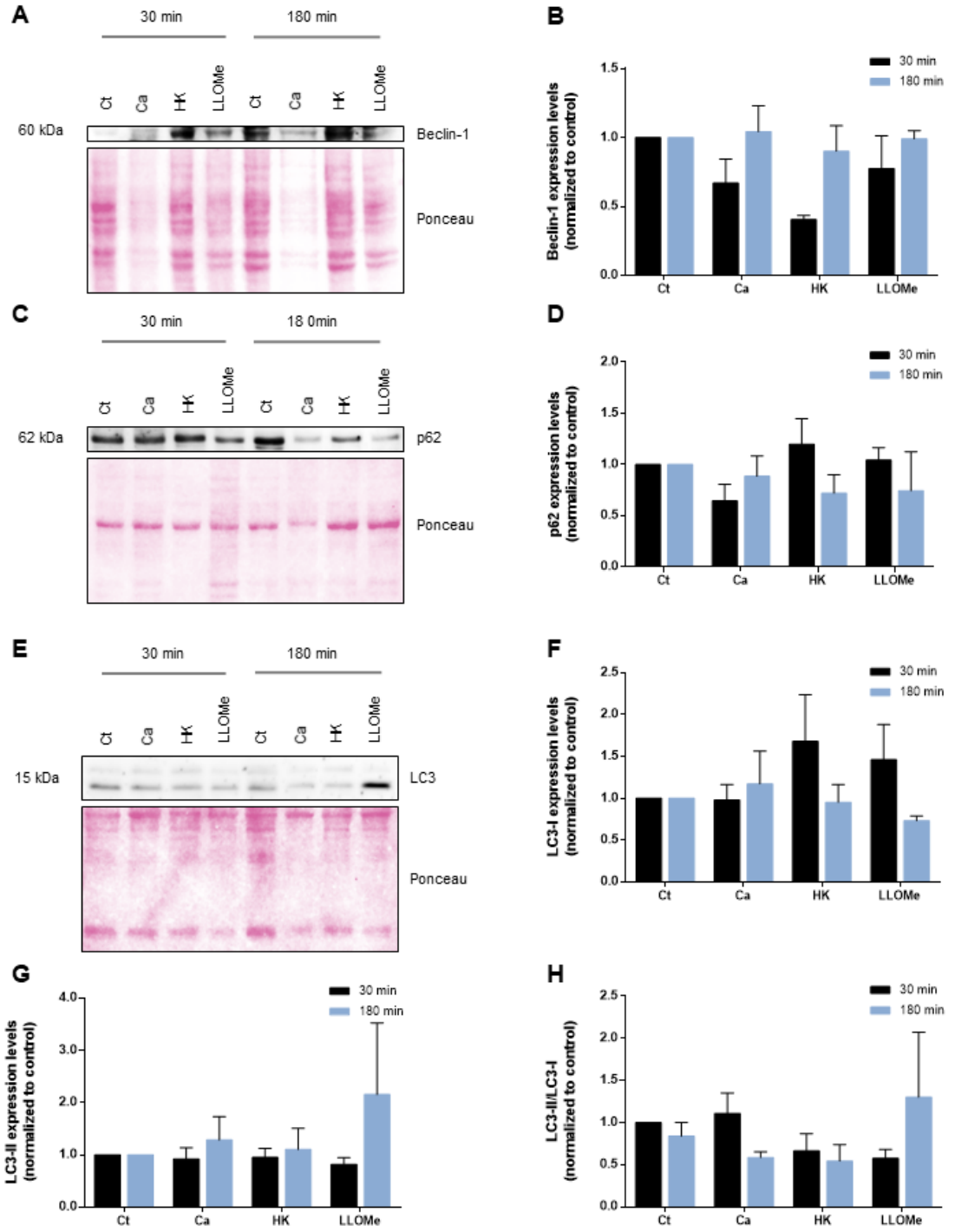

Figura 10 | Autophagy is not significantly affected during macrophages *Candida albicans* infection
(A) Representative immunoblot image and **(B)** quantification of beclin protein total levels upon RAW cells infection with *C. albicans* (Ca) or heat-killed (HK) *C. albicans,* or incubated with 500µM of LLOMe, for 30 or 180 min. Results represent the mean ± SEM from 4 independent experiments. Ponceau was used as loading control. **(C)** Representative image and **(D)** quantification of p62 protein levels upon RAW cells infection with Ca or HK, or incubated with 500µM of LLOMe, for 30 or 180 min. Results represent the mean ± SEM from 4 independent experiments. Ponceau was used as loading control. **(E)** Representative image and quantification **(F-H)** of immunoblot analysis of LC3-I, LC3-II and LC3-II/LC3-I protein levels upon RAW cells infection with Ca or HK, or incubated with 500µM of LLOMe, for 30 or 180 min. Results represent the mean ± SEM from 6 independent experiments. Ponceau was used as loading control.

The results obtained showed that Lamp1 protein levels were not significantly affected during *C. albicans* infection, but nevertheless, a trend for the decrease of Lamp1 levels at 30 min post-infection in macrophages infected with *C. albicans* was observed, which coincides with the yeast-to-hypha transition. In LLOMe treated cells, Lamp1 expression levels were significantly reduced after 30 min of treatment **(Figure 11A and 11B)**. We also performed single cell analysis of Lamp1 total intensity levels through immunofluorescence imaging. In agreement with our immunoblot results, our measurements demonstrated similar intensity values of Lamp1 in macrophages infected for 30 or 180 min post-infection **(Figure 11C)**. Altogether, our findings appear to indicate that both autophagy and *de novo* synthesis of lysosomes are not the primordial defence mechanism upregulated to manage *C. albicans* infection.

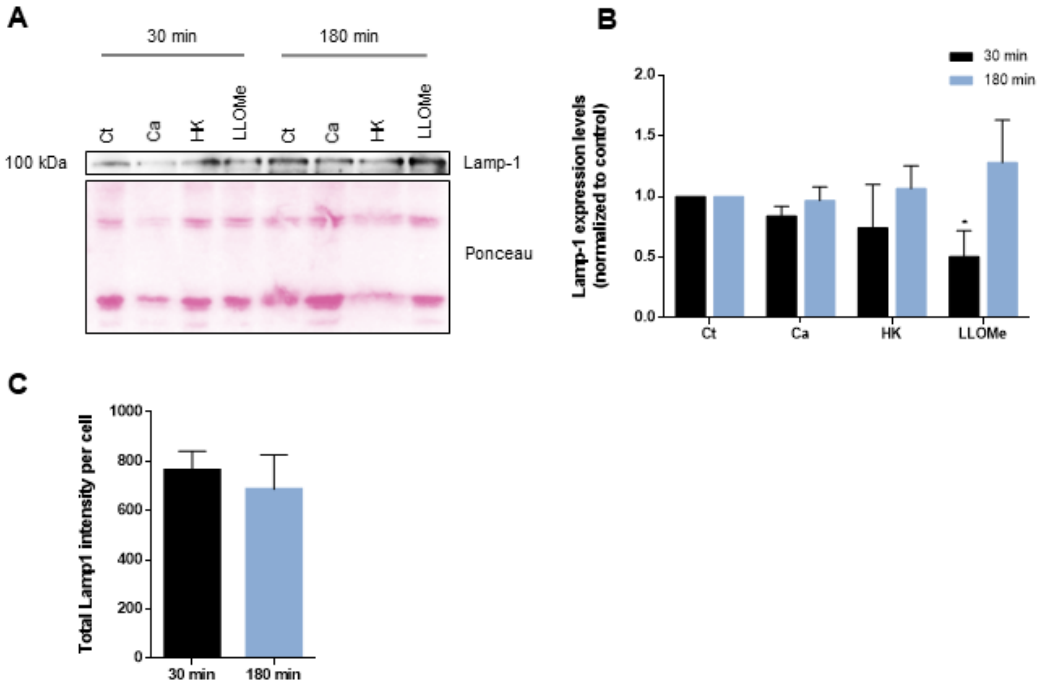

Figura 11 | Lysosomal biogenesis is not significantly affected during macrophages *Candida albicans* infection
(A) Representative immunoblot image and **(B)** quantification of Lamp-1 protein total levels upon RAW cells infection with Ca or HK, or incubated with LLOMe, for 30 or 180min post-infection. The results represent the mean ± SEM from 4 independent experiments. *p*-values were calculated by a one-way ANOVA followed by Dunnett's multiple comparisons test ($*p < 0.05$), compared to Ct 30 min. Ponceau was used as loading control. (C) Single cell analysis of total Lamp1 fluorescence intensity in macrophages cells infected with Ca during 30 or 180 min. The results represent the mean ± SEM from 3 independent experiments. For each condition, at least 6 cells were analysed in each experiments.

4.4. Phagosomal membrane integrity is crucial to the host defence

Impairment of phagosome expansion has been recently reported to facilitate hyphal growth [85]. To further characterize the effect of phagosomal membrane integrity and autophagy in internalized hyphae extension, we treated infected RAW cells with BAPTA-AM, 3-MA and LLOMe. 3-MA was used as an autophagy inhibitor and LLOMe as a positive control for phagolysosome damage. We started by quantifying the number of hyphae per cell and *C. albicans* length in the presence or absence of these compounds **(Figure 12A to 12C)**. Our results demonstrated that all treatments had no significant effect on the number of hyphae per cell. However, and in agreement with the findings of Westman and colleagues [85], there was a trend for the increase of hypha length upon treatment with BAPTA-AM. Interestingly, the same result was obtained with 3MA and LLOMe, with the latter having a more robust increase.

Recently a new host defence mechanism of macrophages against *C. albicans* infection named hyphal folding, was reported [82]. Using actin ring structures localized around the hypha-containing phagosomes, the macrophage induces hyphal folding, consequently damaging the integrity of *C. albicans,* hampering its hypha growth and escape, and facilitating its complete engulfment by the phagosome [82]. In order to understand the impact of phagolysosomal membrane homeostasis on this defence mechanism, we next measured the percentage of hyphal folding on *C. albicans* alone and in presence of the aforementioned compounds **(Figure 12D)**. The results obtained showed that loss of phagosomal integrity and autophagy inhibition significantly decreased hyphal folding capacity of macrophages. LLOMe treatment did not affect the folding capacity of macrophages. Therefore, our results suggest that the integrity of the phagosomal membrane may have a crucial role in this new host response against *C. albicans*.

4.5. Cx43 is present in the expanding phagosomal membranes

In order to unveil new molecular players involved in the progressive response of macrophages to the yeast-to-hypha transition, we performed an analysis of a published dataset (GSE111731). Our main goal was to ascertain the genes implicated in the different stages of the macrophage response to the abnormal phagosome, taking into account the related cellular mechanisms as well as some proteins already described to be involved in the hypha folding process. We also integrated into our analysis published molecular targets involved in actin ring structures from Maxson and

colleagues work [39]. Initially, we compared the different time points progressively: 0-60, 60-120 and 120-240 min, identifying 695, 657 and 235 DEGs (P-Value <0.05), respectively (unpublished results).

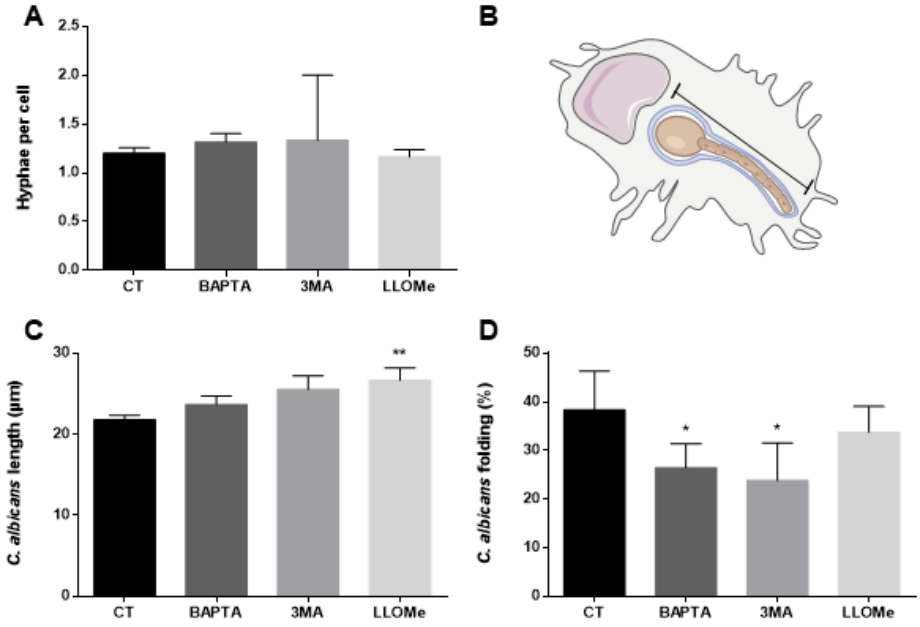

Figura 12 | Integrity of phagosomal membrane impacts *Candida albicans* hyphal growth and folding

(A) Quantification of hyphae per cell, RAW cells were infected with *C. albicans* and treated with vehicle, BAPTA-AM, 3MA or LLOMe for 180 min post-infection. **(B)** Schematic representation of the methodology used for the measurement of *C. albicans* length. **(C)** *C. albicans* length and percentage of hyphal folding **(D)** upon RAW cells infected with *C. albicans* and treated with vehicle, BAPTA-AM, 3MA or LLOMe during 180 min. Results represent the mean ± SEM from 3 independent experiments. At least 15 cells were analysed per condition in each independent experiment. *p*-values were calculated by a one-way ANOVA followed by Dunnett's multiple comparisons test ($*p$ < 0.05; $**p$ <0.01), compared to Ct.

As mentioned earlier, hypha folding is a process that depends on the phagosome vesicle structure and on the migratory capacity of macrophages. Thus, to further disclose new molecular players that could potentiate macrophage capacity to fold hypha, we intersected all the DEGs from cell migration, such as focal adhesion and cell leading edge, and vesicular structures, including endocytic vesicle and lysosomal membrane GO cellular component (CC) terms. The results revealed that 47 DEGs are shared between vesicular trafficking and cell migration related pathways. We then observed the STRING network of these genes, which were clustered in four functional groups: locomotion, focal adhesion, actin filament-based process and endocytosis **(Figure 13A)**. The gene expression profile was found to change during *C. albicans* infection as depicted in **Figure 13B**. Interestingly, we identified the GJA1 gene, which

encodes Cx43, as a putative hit. In the functional analysis of our network, Cx43 was associated with locomotion and actin filament-based processes.

Besides its role in direct intercellular communication, Cx43 has been associated to several non-canonical functions [116], [127]–[129], [138]. Unpublished data from our group shows a recruitment of Cx43 to damaged lysosomes. Considering this, we next investigated the role of Cx43 during *C. albicans* infection. Firstly, we analysed Cx43 distribution in infected RAW cells through fluorescence immunostaining **(Figure 13C)**. The results showed an increase in Cx43 recruitment to phagolysosomes containing *C. albicans* in the hyphal form in comparison to the yeast form. To further validate these results, we assessed the fraction of cellular Cx43 that is recruited to the phagolysosomes containing *C. albicans* **(Figure 13D)**. Our results demonstrated that the length of the internalized *C. albicans* positively correlates with the increase of the phagosomal Cx43 fraction, thus suggesting that hypha elongation promotes Cx43 recruitment to the phagolysosome. We also evaluated the expression levels of Cx43 upon macrophages infection **(Figure 13E and 13F)**. Our results revealed a slight decreased in Cx43 protein levels after 30 min, with expression values recovering near to control levels after 180 min of *C. albicans* infection. Together, these results may suggest a potential role of Cx43 in the cellular response of macrophages to the expanding phagosome containing hypha.

4.6. Overexpression of Cx43 increases hyphal folding

To further elucidate the role of Cx43 during *C. albicans* infection, we started by assessing the number of hyphae per cell, *C. albicans* length and hyphal folding upon treatment of infected RAW cells with Carbenoxolone (CBX), a gap junction inhibitor **(Figure 14A to 14C)**. The results obtained showed that the number of hyphae per cell and *C. albicans* length had no significant changes upon treatment with CBX. However, a significant decrease in the percentage of folded hypha was observed in cells treated with the gap junction inhibitor. Next, we generated a polyclonal RAW cell line overexpressing Cx43 **(Figure 14D to 14F)** and, in order to have a more homogeneous population with the same basal Cx43 levels, we generated four different monoclonal cell lines **(Figure 14G and 14H)**.

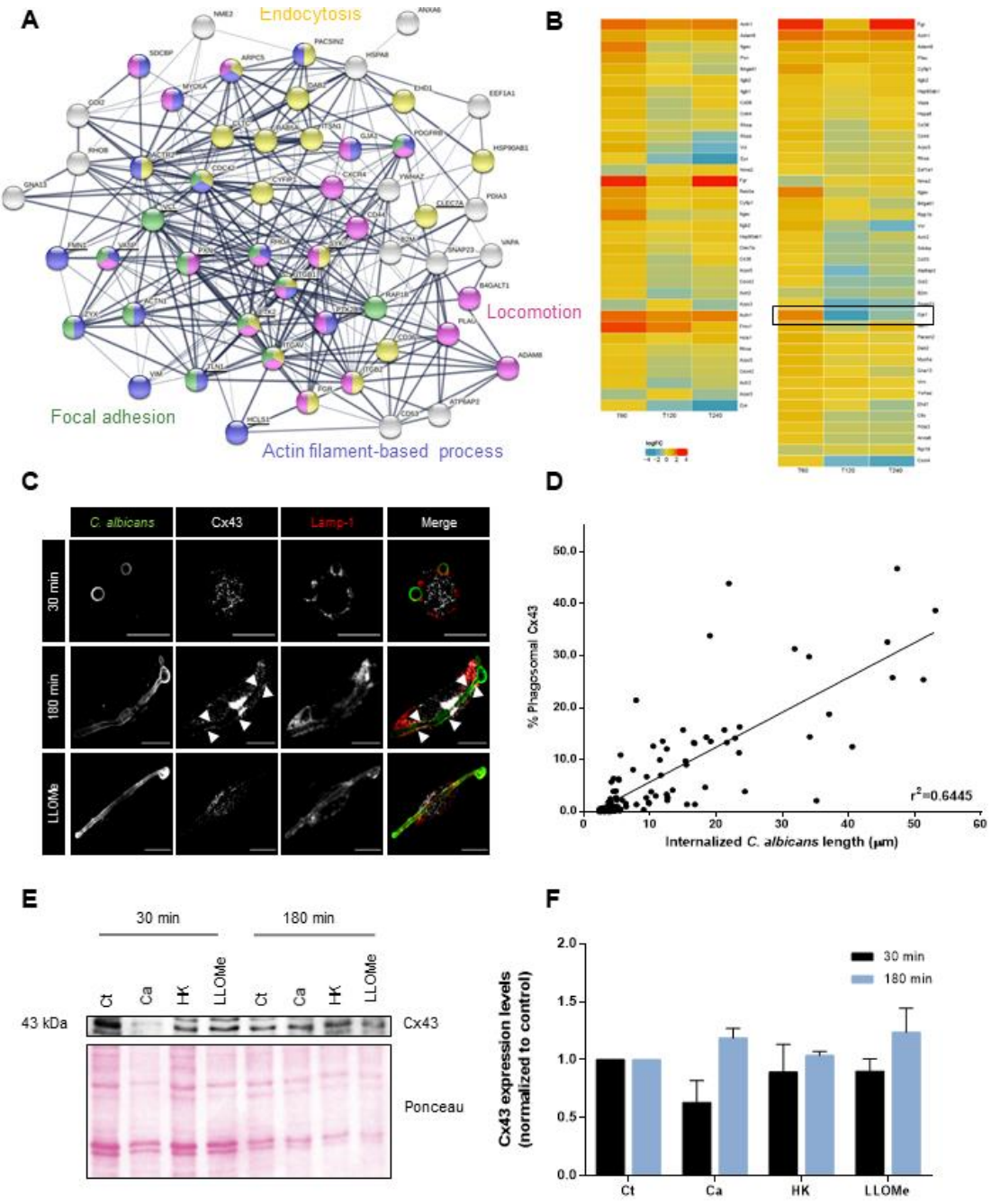

Figura 13 | Cx43 appears as a new molecular player during *Candida albicans* infection in macrophages

(A) Network analysis and functional enrichment of the 47 genes present in the intersection from CC:terms related with cell mobility and vesicular trafficking, combined with the molecular players already described in the literature to have a role on actin-contractile rings surrounding hyphae using STRING database. The functional enrichment of the three main identified clusters is colored in green (focal adhesion), yellow (endocytosis), blue (actin filament-based process) and purple (locomotion). The solid and the dotted lines indicate connection within the same and different cluster respectively [Protein-protein interaction enrichment p-value: < $3x10^{-5}$, strength: > 0.9]. **(B)** Heat map representing the relative expression of the differentially expressed genes presented in (A). **(C)** Representative confocal images of RAW cells infected with *C. albicans*, fixed after 30 or 180 min post-infection, and immunostained for *C. albicans*, Cx43 and Lamp-1. Scale bar, 10 µm. White arrowheads indicate sites of Cx43 accumulation at the phagosome containing hypha. **(D)** Linear regression analysis correlating the length of internalized *C. albicans* and percentage of phagosomal Cx43 quantified as (phagosomal Cx43/total Cx43)*100, in RAW cells. Results were obtained from 3 independent experiments, and at least 15 cells were analysed per experiment. **(E)** Representative image and quantification **(F)** of Cx43 protein total levels upon RAW cells infected with *C.*

albicans (Ca) or heat-killed (HK) *C. albicans,* or incubated with 500µM of LLOMe for 30 or 180 min post-infection. Results represent the mean ± SEM from 3 independent experiments.

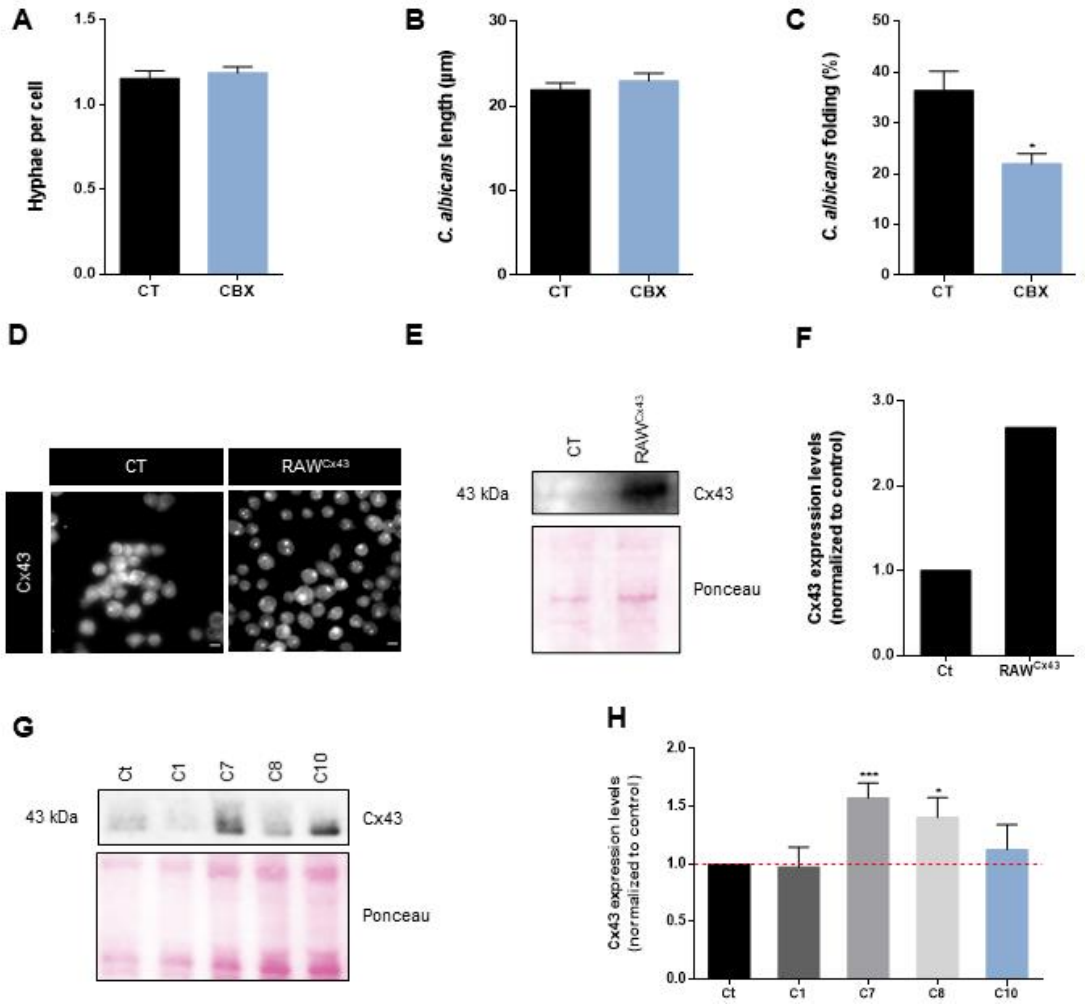

Figura 14 | Inhibition of gap junction affects hyphal folding capacity of infected macrophages. Development of a macrophage cell line overexpression Cx43
Quantification of **(A)** hyphae per cell, **(B)** *C. albicans* length and **(C)** percent of hyphal folding upon RAW cells infected with *C. albicans* and treated with CBX for 180 min post-infection. **(D)** Representative confocal images of control RAW cells and a polyclonal RAW cell line overexpressing Cx43 (RAW^{Cx43}) immunostained for Cx43. Scale bar, 10 µm. **(E-H)** Cx43 overexpression was verified by immunoblotting, using Ponceau as a loading control. Results in **(C)** represent mean ± SEM from 4 independent experiments. At least 30 cells were analysed per condition in each independent experiment. *p*-values were calculated by a one-way ANOVA followed by Dunnett's multiple comparisons test ($*p < 0.05$), compated to Ct. Results in **(F)** represent 1 independent experiment. Results in **(H)** are mean ± SEM from 3 independent experiments. *p*-values were assessed by a one-way ANOVA followed by Dunnett's multiple comparisons test ($*p < 0.05$; $***p$ <0.001), compared to Ct.

Our results showed that colonies (C) 7 and 8 presented the highest expression levels of Cx43. Using these two monoclonal cell lines we started by investigating whether overexpression of Cx43 could affect the phagocytic capacity of macrophages. For this, we performed a phagocytic assay using IgG-opsonized beads. As expected, macrophages presented an increase in phagocytic index from 30 to 180 min of

incubation time **(Figure 15A and 15B)**. Notably, our results also indicated that C7 and C8 Cx43-overexpressing macrophages showed an increase in phagocytic index after 180 min of cell incubation with beads, when compared with control cells. The phagocytic capacity of macrophages in *C. albicans* internalization was also investigated. Our results also revealed an increase in the internalized *C. albicans* (yeast and hyphal forms) in C8 macrophages **(Figure 15C)**. However, a diminished phagocytosis capacity was observed in C7 macrophages. Interestingly, we found a significant increase in the numbers of hyphae per cell in C8 and C10 **(Figure 15D)**. Furthermore, C7 and C10 significantly increased *C. albicans* length **(Figure 15E)**. Additionally, we found a significant increase of hyphal folding in the Cx43 overexpressing cells, with significant difference for C7 macrophage cells **(Figure 15F)**. In order to understand whether Cx43 overexpression could counteract the effects of compromised phagosomal membrane integrity, we next tested the response of the monoclonal cell lines overexpressing Cx43 to expanding hypha in the presence of BAPTA-AM or LLOMe. Our data demonstrated that the presence of BAPTA-AM seemed to increase *C. albicans* length and hyphal folding in C7-overexpressing Cx43 line **(Figure 15G and 15H).** Additionally, LLOMe treatment appeared to slightly decrease *C. albicans* length and folded hyphae in Cx43 overexpressing cells **(Figure 15I and 15J)**.

As mentioned earlier, actin filaments are essential to promote hyphal folding. In cardiac cells it was shown that the GJA1-20k isoform promotes actin polymerization and stabilizes filamentous actin [139]. Thus, considering the observed effects of Cx43 in *C. albicans* folding, we next investigated the recruitment of Cx43 to the actin rings surrounding the hypha. Notably, our preliminary results showed a high colocalization of Cx43 with actin rings **(Figure 15K)**. Furthermore, we proposed to investigate whether Cx43 localized at the actin rings could contribute to the recruitment of complexes involved in actin nucleation, such as Arp2/3 complex. Thus, we evaluated the colocalization of Cx43 and Arp2 at actin rings in *C. albicans* hypha through immunofluorescence imaging. Interestingly, results showed a robust colocalization of Cx43 and Arp2 around the actin ring structures, which are localized around the phagolysosomes containing *C. albicans* **(Figure 15L)**. Altogether, these findings suggest that Cx43 might have an important role during the hyphal folding mechanism of the macrophage by contributing to anchor some complexes involved in the process of actin nucleation.

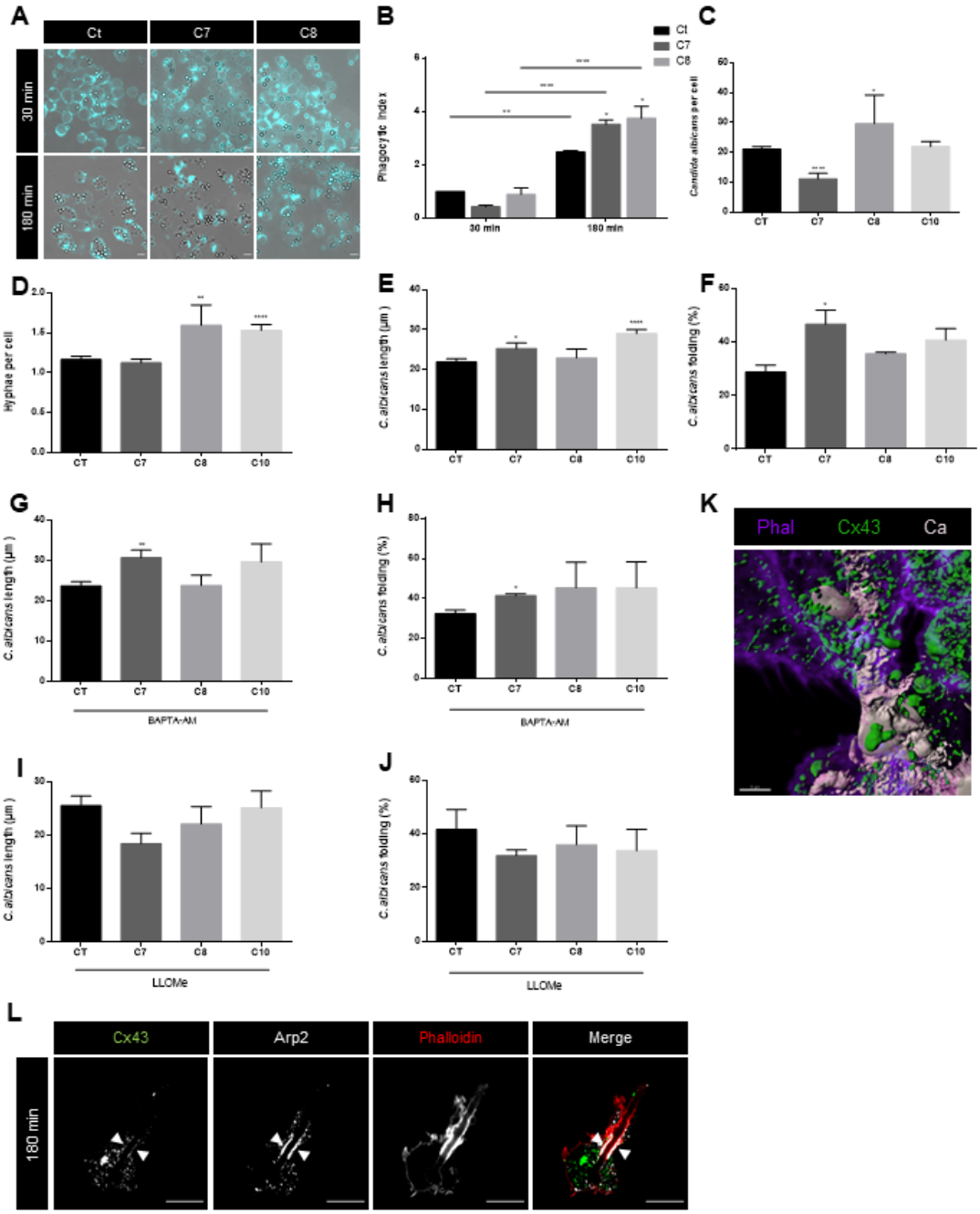

Figura 15 | Cx43 slightly increases phagocytic capacity and promotes hypha folding
(A) Representative fluorescence and bright field images of control RAW cells and two monoclonal cell lines overexpressing Cx43 showing phagocyted beads loaded for 30 or 180 min post-incubation. Non-internalized beads were immunostained (cyan beads). Scale bar, 10 µm. **(B)** Phagocytic index of control RAW cells and two monoclonal cell lines overexpressing Cx43. Results represent the mean ± SEM from 3 independent experiments. At least 10 cells were analysed per condition in each independent experiment. *p*-values were calculated by two-way ANOVA followed by Tukey's multiple comparison test ($*p$ < 0.05; $**p$ <0.01; $****p$ <0.0001), compared to 30 min. **(D-F)** Quantification of **(D)** hyphae per cell, **(E)** *C. albicans* length and **(F)** percent of hyphal folding upon control RAW cells and three monoclonal cell lines overexpressing Cx43, fixed 180 min post-infection. Results represent the mean ± SEM from 3 independent experiments. At least 5 cells were analysed per condition in each independent experiment. *p*-values were calculated by a one-way ANOVA followed by Dunnett's multiple comparisons test ($*p$ < 0.05; $**p$ <0.01; $****p$ <0.0001). **(G-H)** Quantification of the **(G)** *C. albicans* length and **(H)** percent of hyphal folding upon control RAW cells and three monoclonal cell lines overexpressing Cx43 treated with BAPTA-AM, for 180 min post-infection. Results represent the mean ± SEM from 3 independent experiments. At least 5 cells

were analysed per condition and independent experiment. *p*-values were calculated by a one-way ANOVA followed by Dunnett's multiple comparisons test ($*p$ < 0.05; $**p$ <0.01), compared to Ct. **(I-J)** Quantification of the **(I)** *C. albicans* length and **(J)** percent of hyphal folding in control RAW cells and three monoclonal cell lines overexpressing Cx43 treated with LLOMe, for 180 min post-infection. Results represent the mean ± SEM from 3 independent experiments. At least 5 cells were analysed per condition in each independent experiment. **(K)** Representative 3-dimensional image of a RAW cell infected with *C. albicans* for 180 min, and immunostained for Cx43 (green), *C. albicans* (beige) and Phalloidin (purple), reconstructed using Imaris software. Scale bar, 3 µm. **(L)** Representative confocal images of RAW cells infected with *C. albicans* during 180 min, and immunostained for Cx43, Arp2 and Phalloidin. Scale bar, 10 µm. White arrowheads indicate sites of Cx43 and Arp2 accumulation in the actin rings.

Discussion

5. Discussion

Phagolysosomal function is crucial to maintain the hostile internal environment required for *C. albicans* clearance from the host [85]. *C. albicans* can grow up to several µm per hour inside the macrophage [81], which can compromise the integrity of the phagosomal membrane. Recently, impairment of phagosomal expansion, by inhibiting Ca^{2+}-dependent lysosomal fusion with phagosomes, was shown to induce membrane rupture, which ultimately facilitates the escape of *C. albicans* from the macrophage [85]. Several emerging studies disclosing the cellular response to injured lysosomes demonstrated that an initial Ca^{2+}-dependent response is important for the recruitment of ESCRT machinery and consequent repair of limited membrane disruptions (reviewed by Papadopoulos, Kravic, & Meyer, 2020; Papadopoulos & Meyer, 2017). Injury-triggered influx of Ca^{2+} causes accumulation of PDCD6 (also known as ALG-2), a Ca^{2+} sensor, at the site of injury, which recruits the ESCRT-III binding protein, Alix. Subsequently, Alix recruits components of the ESCRT machinery that mediate membrane repair by budding and fission of the damaged membrane area [(reviewed in [140]]. Interestingly, the ESCRT machinery has also been demonstrated to mediate repair of the plasma membrane [141], [142], nuclear envelope [143]–[146] and pathogen-induced phagosomal damage [99], [103], [147], raising the possibility that ESCRT machinery might also respond to *C. albicans*-induced phagosomal damage. Indeed, our results showed for the first time that the recruitment of Alix and Tsg101 to hypha-containing phagolysosome is dependent on Ca^{2+} release from the phagosome. Although, further molecular studies are required, our data suggests that, similarly to the repair of chemical-induced lysosomal damage, an initial Ca^{2+} influx from injured expanding phagolysosomes may also trigger the assembly of ESCRT machinery, contributing to the detection and repair of the disrupted membrane. These findings are in line with very recent work that suggested the involvement of two Ca^{2+}-dependent repair mechanisms during *C. albicans* infection of epithelial cells. Ruptured membrane regions were shown to be eliminated through an Alg-2/ALIX/ESCRT-III-dependent blebbing process and a repair of plasmalemmal vesicles induced via exocytic insertion of lysosomal membranes [106]. Notably, some pathogens, such as *Mycobacterium tuberculosis*, have their own effectors to impair ESCRT recruitment to sites of endolysosomal damage, thus preventing disrupted endolysosomes to be repaired or eliminated [103]. Conversely, little is known about the repair mechanisms in the context of hypha growth inside macrophage phagolysosomes. Moreover, in macrophages infected with *C. albicans*, LRRK2 was demonstrated to be activated, promoting the recruitment of the Rab GTPase, Rab8A and the ESCRT-III component CHMP4B to

damaged endolysosomes thereby inducing ESCRT-mediated repair [104], [105]. Nevertheless, these results were controversial, since the recruitment of the repair machinery was only demonstrated in yeast-containing phagolysosomes and this *C. albicans* form, related to bloodstream dissemination, was never reported to induce membrane damage in macrophages [22], [24], [148].

Lysophagy activation has been observed upon unrepairable lysosomal damage [93], [104]. Although, activation of lysophagy as part of the host defence mechanism has been already reported in macrophages infected by other pathogens, such as *M. tuberculosis* [137], [149], this process is still poorly characterized for *C. albicans* infection. Previously, Gal3 was shown to be distributed to the ruptured sites of the phagosomes containing the expanding hypha [85]. Upon lysosomal damage, Gal3 interacts with Alix and the autophagy-associated E3 ubiquitin ligase Trim16 [102], [137] orchestrating the destiny of damaged membranes to repair or autophagy [102]. Our results reveal only a slight recruitment of Gal3 to the phagosome containing *C. albicans*. Interestingly, a more preeminent recruitment of Trim16 to the *C. albicans*-containing phagolysosome was observed. Despite being a classical component of the lysophagy process [137], Trim16 was also described to be involved in inflammasome regulation [150], [151]. In response to lysosomal damage, Trim16 was shown to interact with IL-1β, mediating IL-1β recruitment to the autophagosome [151]. This cytokine plays a key role in inflammation triggered by lysosomotropic agents [152]–[154] and also in macrophages infected with *C. albicans*. NLRP3 inflammasome, which mediates IL-1β production, was described to be activated upon *C. albicans* infection in macrophages [68], [155]–[158] as the major consequence of phagosomal rupture [85]. Activation of this multi-component protein complex occurs in response to cytosolic presence of lysosomal content, which will trigger the activation of caspase-1 and the secretion of pro-inflammatory cytokines IL-1β and interleukin 18 (IL-18), which can ultimately lead to the macrophage's death through pyroptosis (early inflammasome-dependent cell death) [66], [85]. Therefore, the observed increase in Trim16 recruitment to hypha-containing phagosomes can be related with its involvement in the inflammatory process of the macrophages infected by *C. albicans.* Additionally, Trim proteins directly regulate the autophagy machinery, being able to associate with both Ulk1 and Beclin1, anchoring the assembly of these factors in a complex to promote their activation through K63-linked polyubiquitination [150], [159]. In macrophages infected with *M. tuberculosis* it was demonstrated that Ub directly binds to *M. tuberculosis* triggering selective autophagy. Similar to Gal3, we only detected a slight increase in Ub recruitment to the *C. albicans*-containing phagolysosomes. Accordingly,

we also did not observe any significant effect on autophagic activity in the infected macrophages. Even though previous findings have demonstrated the presence of LC3 on *C. albicans* containing phagosomes [43], it has also been reported that *C. albicans* induces little [160], [161], if any [162] recruitment of LC3 to the phagosome. Thus, the role of autophagy during *C. albicans* infection still requires further in-depth investigation.

To prevent phagosome rupture during hyphal growth, lysosomal fusion with the phagosome is induced through a Ca^{2+}-dependent process [85]. Infected macrophages display increased nuclear translocation of TFEB, a master regulator of lysosomal biogenesis [110], suggesting a stimulation of *de novo* synthesis of lysosomes upon *C. albicans* infection in order to replace the consumed lysosomal pool [85]. Unexpectedly, our results did not show increased levels of Lamp1, one of the most abundant lysosomal transmembrane proteins [88], during the infection time. In accordance with our finding, RNAseq analysis of cell sorted *C. albicans* infected macrophages [27] and our progressive analysis of this dataset also did not reveal increases in the expression of CLEAR genes over the infection time (unpublished data). These results might suggest that the biogenesis of new vesicles may not be the main source of new membranes to deal with hyphal formation. In this scenario, it is conceivable that macrophages implement other alternative strategies upon hyphal formation to overcome the infection.

Very recent work has described the folding of fungal hypha as a new antimicrobial response of macrophages [82]. Actin-contractile ring structures were found surrounding the phagosomes containing hypha causing folding, damage and consequent impairment of their viability [82]. The authors also suggested that effective hyphal folding is dependent on macrophages generating mechanical forces via their cytoskeletal network responsible for cell migration, thus asserting cell motility as part of antimicrobial strategies. However, the effect of phagosomal membrane damage in this context was not addressed. Thus, our data contributed to further characterize how the process of hyphal folding is affected by compromised phagolysosomal membrane integrity. We found that the folding rate of *C. albicans* decreased significantly upon Ca^{2+} chelation and inhibition of autophagy, suggesting that phagosomal membrane integrity may be required to potentiate the hyphal folding mechanism. Actin polymerization, Myosin II activity and vasodilator-stimulated phosphoprotein (VASP) were demonstrated to be crucial for hyphal folding, as well as the expression of Dectin-1 and β2 integrin, fungal pattern-recognition receptors which interact with β-glucan [82]. Furthermore, Dectin-1 has also been reported to potentiate the formation of actin cuffs

surrounding frustrated phagosomes that are attempting to engulf large fungal hyphae, in epithelial cells [39]. However, the specific signals and the receptors that can be involved in anchoring actin structures around the hypha-containing phagosome remains to be elucidated.

Macrophages regulate subsets of genes upon *C. albicans* exposure and phagocytosis [26], [27]. As briefly mentioned above, through a robust technique to separate and analyze *C. albicans* and infected macrophage subpopulation in different stages through cell sorting and RNAseq [27], an increase in the number of DEGs in both macrophages and *C. albicans* was demonstrated only after 60 min infection. In phagocyted *C. albicans*, an increase in the expression of genes involved in the core filamentation response was observed after 120 min of infection, indicating an activation of yeast-to-hypha transition at this time point. Concomitantly, macrophages also presented a transcriptional shift during the infection period, with an upregulation of endocytosis related genes in the early stage of the phagocytosis, which decline over infection time [27]. In order to unveil new molecular mechanisms involved in the progressive response of macrophages to the damaged phagosomes induced by yeast-to-hypha transition, we performed an analysis of this published dataset (GSE111731). Our main goal was to establish the mechanisms and players implicated in different stages of the macrophage response to the abnormal phagosome, integrating in our analysis published molecular targets. Our integrative analysis of the DEGs involved in cellular components related to the hypha folding process and contractile actin ring assembly, identified gap junction gene (GJA1), a gene encoding the Cx43 protein, as a putative hit in this infection. Interestingly, unpublished data from our group has demonstrated that upon lysosomal damage, Cx43 is recruited to the injured vesicles promoting lysosomal exocytosis. Within the context of membrane proteins, Cx43 presents a short half-life [163], [164], being continuously delivered to the lysosome for degradation [165]. Thus, Cx43 localization to the lysosome has always been interpreted as a consequence of its degradation process, and a role for the protein in lysosomal homeostasis has never been reported. In this work, we clearly showed that Cx43 is present in phagosomes containing hypha and in actin ring sites, potentiating hyphal folding of *C. albicans*. The role of Cx43 in actin organization and dynamics is still poorly understood. Nevertheless, the GJA1-20k isoform was shown to induce actin polymerization and stabilize polymerized filamentous actin [139]. Furthermore, ZO-1 was demonstrated to be associated with Cx43 in the modulation of focal adhesions and the actin cytoskeleton [166], [167]. Interestingly, ZO-1 recruitment to the site of cytoskeleton reorganization and its colocalization with newly formed actin filaments

was observed upon *C. albicans* invasion, in epithelial cells [168]. Thus, our results contribute to better understand the Cx43-actin interaction upon *C. albicans* infection.

Actin structures around partially internalized *C. albicans* were firstly described as a stabilizer of frustrated phagosomes [39]. In these frustrated phagosomes, actin assembly was reported to be SYK, PYK2/FAK and formin-dependent. Nevertheless, the molecular mechanism involved in actin polymerization of the ring structure responsible for the folding of expanding hypha inside the phagosome remains elusive. Our gene interacting analysis identified Actin-related protein 2/3 complex subunit 5 (ARCP5), a component of the Arp2/3 complex, and Actin-related protein 2 (ACTR2), which functions as an ATP-binding component of the Arp2/3 complex, to be involved in cellular components related with the folding process. Indeed, our results showed Arp2 recruitment to the actin ring of folded hypha. Surprisingly, our results also showed a colocalization of Cx43 with Arp2 at actin rings sites. Although the interaction of Cx43 and Arp2/3 has never been reported, Pannexin1 (Panx1), a channel protein with similar structure to connexins, has been shown to associate with the Arp2/3 complex. Panx1, which is expressed in doublecortin-positive migrating neuroblasts in adult brain, was shown to regulate neural stem and progenitor cell behaviours through its interaction with Arp3, a major part of the Arp2/3 complex, contributing to cell proliferation, neurogenesis and cell migration [169]. Even though our results are only preliminary, requiring further confirmation, we speculate that Arp2 and Cx43 are both involved in the hyphal folding mechanism, and modulation of these proteins could potentiate macrophage response to *C. albicans* infection. Altogether, the current findings suggest that Cx43 may have a crucial role on the macrophage response to *C. albicans* infection, particularly in the hyphal folding mechanism, contributing to a better understanding of *C. albicans* infection of macrophages.

Concluding remarks and future perspectives

6. Concluding remarks and future perspectives

Although, the recent advances in therapeutic interventions, the antifungal resistance is an emerging problem worldwide. Therefore, with this work we intend to contribute for a better understanding of the recent molecular mechanisms involved in macrophage response to hypha, unveiling a potential role of Cx43 during the molecular response to the expanding hypha inside the phagolysosome. Moreover, our results revealed that maintenance of the phagosomal membrane integrity is essential to control the hyphal growth and to potentiate the macrophage folding capacity. Furthermore, our work also demonstrated that Cx43 is present in actin-contractile structures and its modulation appears to affect the hypha folding capacity of macrophages. The proposed model of this thesis is depicted in **Figure 16.** Nevertheless, further experiments are required to validate and deeper investigate some of our achievements. To further evaluate the effects of repair capacity on the macrophage response to expanding hypha, it will be crucial to modulate the levels of these components, such as Alix levels, and measure the length and the hypha folding percentage in infected cells. In addition, a more detailed analysis of Cx43 action upon *C. albicans* infection, envisioning its role during hypha-induced phagosome damage, as well as its effect in actin-contractile ring assembly, are essential step toward a deeper comprehensive understanding about the host response. In order to understand involvement of Cx43 in hypha folding, it will be essential to perform immunoprecipitation assays and analyze the interaction between Cx43 and *actin*-related *proteins*, such as Arp2, upon different infection time with *C. albicans*. Moreover, to better elucidate whether autophagy is being modulated, playing an important function during the cellular response to the expanding hypha, the presence of autophagic associated proteins in the hypha-containing phagosome should also be addressed, as LC3-II or p62.

Altogether, this master thesis sheds a new light on the impact of the phagosomal membrane integrity, autophagy, lysosomal biogenesis and some new mechanistic targets involved in macrophage-*C. albicans* interaction. We hope to contribute to the discover of new molecular players during infection and ultimately to design targeted therapeutic approaches modulating the host response, without affecting other important innate immune responses.

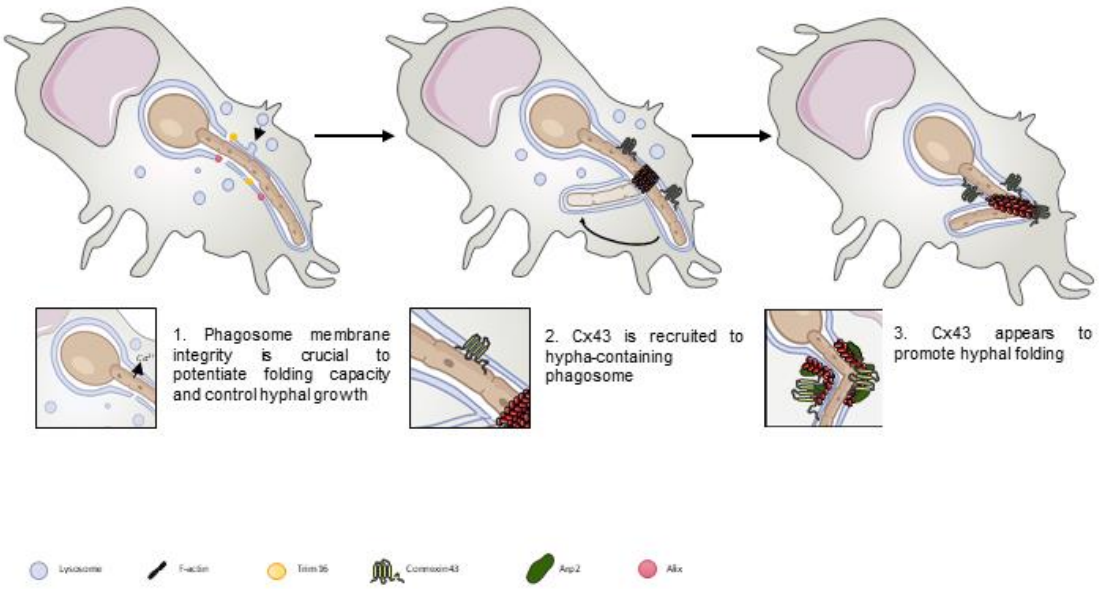

Figura 16 | Schematic model of Cx43 as a new player in *Candida albicans* infection of macrophages
Maintenance of the phagosomal membrane integrity is essential to control the hyphal growth and potentiate folding capacity of the macrophage, promoting an additional defence and avoiding *C. albicans* escape from the ruptured phagosome and ultimately from the macrophage itself. In addition, our work showed that Cx43 is recruited to the phagosome containing hypha and its protein levels seem to affect hypha folding. Interestingly, Cx43 and Arp2 are present in the F-actin contractile rings around the phagosomes containing the hypha and seem to be recruited to the folding sites, suggesting a new role of Cx43 and Arp2 in *C. albicans* folding process.

References

7. References

[1] P. G. Pappas, M. S. Lionakis, M. C. Arendrup, L. Ostrosky-Zeichner, and B. J. Kullberg, “Invasive candidiasis,” *Nat. Rev. Dis. Prim.*, vol. 4, no. May, pp. 1–20, 2018.

[2] F. Bongomin, S. Gago, R. O. Oladele, and D. W. Denning, “Global and multi-national prevalence of fungal diseases—estimate precision,” *J. Fungi*, vol. 3, no. 4, 2017.

[3] M. A. Pfaller and D. J. Diekema, “Epidemiology of invasive candidiasis: A persistent public health problem,” *Clin. Microbiol. Rev.*, vol. 20, no. 1, pp. 133–163, 2007.

[4] E. Bouza and P. Muñoz, “Epidemiology of candidemia in intensive care units,” *Int. J. Antimicrob. Agents*, vol. 32, no. SUPPL. 2, pp. 87–91, 2008.

[5] M. Razzaghi-Abyaneh *et al.*, “Species distribution and antifungal susceptibility of Candida spp. isolated from superficial candidiasis in outpatients in Iran,” *J. Mycol. Med.*, vol. 24, no. 2, pp. e43–e50, 2014.

[6] K. E. Pristov and M. A. Ghannoum, “Resistance of Candida to azoles and echinocandins worldwide,” *Clin. Microbiol. Infect.*, vol. 25, no. 7, pp. 792–798, 2019.

[7] G. D. Brown, D. W. Denning, N. A. R. Gow, S. M. Levitz, M. G. Netea, and T. C. White, “Hidden killers: Human fungal infections,” *Sci. Transl. Med.*, vol. 4, no. 165, 2012.

[8] B. J. Kullberg and M. C. Arendrup, “Invasive candidiasis,” *N. Engl. J. Med.*, vol. 4, pp. 1445–1456, 2018.

[9] S. S. Magill *et al.*, “Multistate Point-Prevalence Survey of Health Care–Associated Infections,” *N. Engl. J. Med.*, vol. 370, no. 13, pp. 1198–1208, 2014.

[10] T. P. McCarty and P. G. Pappas, “Invasive Candidiasis,” *Infect. Dis. Clin. North Am.*, vol. 30, no. 1, pp. 103–124, 2016.

[11] A. Chowdhary, C. Sharma, and J. F. Meis, “Candida auris: A rapidly emerging cause of hospital-acquired multidrug-resistant fungal infections globally,” *PLoS Pathog.*, vol. 13, no. 5, pp. 1–10, 2017.

[12] J. Guinea, “Global trends in the distribution of Candida species causing candidemia,” *Clin. Microbiol. Infect.*, vol. 20, no. 6, pp. 5–10, 2014.

[13] Y. Song, X. Chen, Y. Yan, Z. Wan, W. Liu, and R. Li, “Prevalence and Antifungal Susceptibility of Pathogenic Yeasts in China: A 10-Year Retrospective Study in a Teaching Hospital,” *Front. Microbiol.*, vol. 11, no. July, pp. 1–12, 2020.

[14] C. A. Kumamoto, M. S. Gresnigt, and B. Hube, “The gut, the bad and the harmless: Candida albicans as a commensal and opportunistic pathogen in the intestine,” *Curr. Opin. Microbiol.*, vol. 56, pp. 7–15, 2020.

[15] R. V. De Rosa FG, Garazzino S, Pasero D, Di Perri G, “Invasive candidiasis and candidemia: New guidelines.,” *Minerva Anestesiol.*, vol. 75, no. 7–8, pp. 453–458, 2009.

[16] L. Ostrosky-Zeichner, J. H. Rex, J. Bennett, and B. J. Kullberg, “Deeply invasive candidiasis,” *Infect. Dis. Clin. North Am.*, vol. 16, no. 4, pp. 821–835, 2002.

[17] I. E. Mba and E. I. Nweze, “Mechanism of Candida pathogenesis: revisiting the vital drivers,” *Eur. J. Clin. Microbiol. Infect. Dis.*, vol. 39, no. 10, pp. 1797–1819, 2020.

[18] N. A. R. Gow, F. L. Van De Veerdonk, A. J. P. Brown, and M. G. Netea, “Candida albicans morphogenesis and host defence: Discriminating invasion from colonization,” *Nat. Rev. Microbiol.*, vol. 10, no. 2, pp. 112–122, 2012.

[19] J. Talapko *et al.*, “Candida albicans-the virulence factors and clinical manifestations of infection,” *J. Fungi*, vol. 7, no. 2, pp. 1–19, 2021.

[20] H. J. Lo, J. R. Köhler, B. Didomenico, D. Loebenberg, A. Cacciapuoti, and G. R. Fink, “Nonfilamentous C. albicans mutants are avirulent,” *Cell*, vol. 90, no. 5, pp. 939–949, 1997.

[21] A. M. A. Murad *et al.*, “NRG1 represses yeast-hypha morphogenesis and hypha-specific gene expression in Candida albicans,” *EMBO J.*, vol. 20, no. 17, pp. 4742–4752, 2001.

[22] B. G. Seman *et al.*, “Yeast and Filaments Have Specialized, Independent Activities in a Zebrafish Model of Candida albicans Infection,” *Infect Immun*, pp. 1–16, 2018.

[23] G. Huang, “Regulation of phenotypic transitions in the fungal pathogen Candida albicans,” *Virulence*, vol. 3, no. 3, pp. 251–261, 2012.

[24] P. E. Sudbery, “Growth of Candida albicans hyphae,” *Nat. Rev. Microbiol.*, vol. 9, no. 10, pp. 737–748, 2011.

[25] I. E. Frohner, C. Bourgeois, K. Yatsyk, O. Majer, and K. Kuchler, “Candida albicans cell surface superoxide dismutases degrade host-derived reactive oxygen species to escape innate immune surveillance,” *Mol. Microbiol.*, vol. 71, no. 1, pp. 240–252, 2009.

[26] M. C. Lorenz, J. A. Bender, and G. R. Fink, “Transcriptional response of Candida albicans upon internalization by macrophages,” *Eukaryot. Cell*, vol. 3, no. 5, pp. 1076–1087, 2004.

[27] J. F. Muñoz *et al.*, “Coordinated host-pathogen transcriptional dynamics revealed using sorted subpopulations and single macrophages infected with Candida albicans,” *Nat. Commun.*, vol. 10, no. 1, 2019.

[28] Q. Qian, M. A. Jutila, N. Van Rooijen, and J. E. Cutler, “Elimination of mouse splenic macrophages correlates with increased susceptibility to experimental disseminated candidiasis.,” *J. Immunol.*, vol. 152, no. 10, pp. 5000–8, 1994.

[29] L. Romani, A. Mencacci, E. Cenci, G. Del Sero, F. Bistoni, and P. Puccetti, “An immunoregulatory role for neutrophils in CD4+ T helper subset selection in mice with candidiasis.,” *J. Immunol.*, vol. 158, no. 5, pp. 2356–62, 1997.

[30] E. Fernández-Arenas, C. K. E. Bleck, C. Nombela, C. Gil, G. Griffiths, and R. Diez-Orejas, “Candida albicans actively modulates intracellular membrane trafficking in mouse macrophage phagosomes,” *Cell. Microbiol.*, vol. 11, no. 4, pp. 560–589, 2009.

[31] N. A. R. Gow, J. P. Latge, and C. A. Munro, “The fungal cell wall: Structure, biosynthesis, and function,” *The Fungal Kingdom*, no. 5, pp. 267–292, 2017.

[32] J. C. Kapteyn *et al.*, “The cell wall architecture of Candida albicans wild-type cells and cell wall-defective mutants,” *Mol. Microbiol.*, vol. 35, no. 3, pp. 601–611, 2000.

[33] L. P. Erwig and N. A. R. Gow, “Interactions of fungal pathogens with

phagocytes," *Nat. Rev. Microbiol.*, vol. 14, no. 3, pp. 163–176, 2016.

[34] P. J. Mumby, J. R. M. Chisholm, C. D. Clark, J. D. Hedley, and J. Jaubert, "A new receptor for beta-glucans," *Nature*, vol. 413, no. 6851, p. 36, 2001.

[35] M. G. Netea, G. D. Brown, B. J. Kullberg, and N. A. R. Gow, "An integrated model of the recognition of Candida albicans by the innate immune system," *Nat. Rev. Microbiol.*, vol. 6, no. 1, pp. 67–78, 2008.

[36] H. Tabata, H. Morita, H. Kaji, K. Tohyama, and Y. Tohyama, "Syk facilitates phagosome-lysosome fusion by regulating actin-remodeling in complement-mediated phagocytosis," *Sci. Rep.*, vol. 10, no. 1, pp. 1–16, 2020.

[37] S. L. Sherrington *et al.*, "Adaptation of Candida albicans to environmental pH induces cell wall remodelling and enhances innate immune recognition," *PLoS Pathog.*, vol. 13, no. 5, pp. 1–28, 2017.

[38] L. E. Lewis *et al.*, "Stage specific assessment of Candida albicans phagocytosis by macrophages identifies cell wall composition and morphogenesis as key determinants," *PLoS Pathog.*, vol. 8, no. 3, 2012.

[39] M. E. Maxson, X. Naj, T. R. O'Meara, J. D. Plumb, L. E. Cowen, and S. Grinstein, "Integrin-based diffusion barrier separates membrane domains enabling the formation of microbiostatic frustrated phagosomes," *Elife*, vol. 7, pp. 1–37, 2018.

[40] R. Levin, S. Grinstein, and D. Schlam, "Phosphoinositides in phagocytosis and macropinocytosis," *Biochim. Biophys. Acta - Mol. Cell Biol. Lipids*, vol. 1851, no. 6, pp. 805–823, 2015.

[41] R. J. Botelho *et al.*, "Localized biphasic changes in phosphatidylinositol-4,5-bisphosphate at sites of phagocytosis," *J. Cell Biol.*, vol. 151, no. 7, pp. 1353–1367, 2000.

[42] J. Westman, S. Grinstein, and M. E. Maxson, "Revisiting the role of calcium in phagosome formation and maturation," *J. Leukoc. Biol.*, vol. 106, no. 4, pp. 837–851, 2019.

[43] A. M. Nicola *et al.*, "Macrophage autophagy in immunity to Cryptococcus neoformans and Candida albicans," *Infect. Immun.*, vol. 80, no. 9, pp. 3065–

3076, 2012.

[44] L. A. Ligeon *et al.*, “Oxidation inhibits autophagy protein deconjugation from phagosomes to sustain MHC class II restricted antigen presentation,” *Nat. Commun.*, vol. 12, no. 1, pp. 1–13, 2021.

[45] L. S. Mayorga, F. Bertini, and P. D. Stahl, “Fusion of newly formed phagosomes with endosomes in intact cells and in a cell-free system,” *J. Biol. Chem.*, vol. 266, no. 10, pp. 6511–6517, 1991.

[46] N. Ghosh and R. Maxfield, “Endocytosis,” *Physiol Rev*, vol. 77, no. 3, pp. 759–803, 1997.

[47] R. Levin, S. Grinstein, and J. Canton, “The life cycle of phagosomes: formation, maturation, and resolution,” *Immunol. Rev.*, vol. 273, no. 1, pp. 156–179, 2016.

[48] C. Bucci *et al.*, “The small GTPase rab5 functions as a regulatory factor in the early endocytic pathway,” *Cell*, vol. 70, no. 5, pp. 715–728, 1992.

[49] H. M. McBride, V. Rybin, C. Murphy, A. Giner, R. Teasdale, and M. Zerial, “Oligomeric complexes link Rab5 effectors with NSF and drive membrane fusion via interactions between EEA1 and syntaxin 13,” *Cell*, vol. 98, no. 3, pp. 377–386, 1999.

[50] A. Simonsen, J. M. Gaullier, A. D’Arrigo, and H. Stenmark, “The Rab5 effector EEA1 interacts directly with syntaxin-6,” *J. Biol. Chem.*, vol. 274, no. 41, pp. 28857–28860, 1999.

[51] R. S. Flannagan, V. Jaumouillé, and S. Grinstein, “The cell biology of phagocytosis,” *Annu. Rev. Pathol. Mech. Dis.*, vol. 7, pp. 61–98, 2012.

[52] J. M. Kinchen and K. S. Ravichandran, “Phagosome maturation: Going through the acid test,” *Nat. Rev. Mol. Cell Biol.*, vol. 9, no. 10, pp. 781–795, 2008.

[53] B. M. Babior, “NADPH oxidase,” *Curr. Opin. Immunol.*, vol. 16, no. 1, pp. 42–47, 2004.

[54] J. A. Mindell, “Lysosomal acidification mechanisms,” *Annu. Rev. Physiol.*, vol. 74, pp. 69–86, 2012.

[55] G. F. W. Walpole, S. Grinstein, and J. Westman, “The role of lipids in host-

pathogen interactions," *IUBMB Life*, pp. 384–392, 2018.

[56] T. Hiroyuki and T. Yumi, "Protein-Tyrosine Kinase, Syk Accelerates Phagosome Maturation by Depolymerizing F-Actin in Complement-Mediated Phagocytosis," *FASEB J.*, 2020.

[57] Y. Shi *et al.*, "Protein-tyrosine kinase Syk is required for pathogen engulfment in complement-mediated phagocytosis," *Blood*, vol. 107, no. 11, pp. 4554–4562, 2006.

[58] B. Okai, N. Lyall, N. A. R. Gow, J. M. Bain, and L. P. Erwig, "Rab14 regulates maturation of macrophage phagosomes containing the fungal pathogen Candida albicans and outcome of the host-pathogen interaction," *Infect. Immun.*, vol. 83, no. 4, pp. 1523–1535, 2015.

[59] A. Haas, "The phagosome: Compartment with a license to kill," *Traffic*, vol. 8, no. 4, pp. 311–330, 2007.

[60] R. Káposzta, L. Maródi, M. Hollinshead, S. Gordon, and R. P. Da Silva, "Rapid recruitment of late endosomes and lysosomes in mouse macrophages ingesting Candida albicans," *J. Cell Sci.*, vol. 112, no. 19, pp. 3237–3248, 1999.

[61] J. E. Strasser, S. L. Newman, G. M. Ciraolo, R. E. Morris, M. L. Howell, and G. E. Dean, "Regulation of the macrophage vacuolar ATPase and phagosome-lysosome fusion by Histoplasma capsulatum.," *J. Immunol.*, vol. 162, no. 10, pp. 6148–54, 1999.

[62] S. C. Tucker and A. Casadevall, "Replication of Cryptococcus neoformans in macrophages is accompanied by phagosomal permeabilization and accumulation of vesicles containing polysaccharide in the cytoplasm," *Proc. Natl. Acad. Sci. U. S. A.*, vol. 99, no. 5, pp. 3165–3170, 2002.

[63] O. Ibrahim-Granet *et al.*, "Phagocytosis and intracellular fate of Aspergillus fumigatus conidia in alveolar macrophages," *Infect. Immun.*, vol. 71, no. 2, pp. 891–903, 2003.

[64] S. Ghosh *et al.*, "Arginine-Induced germ tube formation in Candida albicans is essential for escape from murine macrophage line RAW 264.7," *Infect. Immun.*, vol. 77, no. 4, pp. 1596–1605, 2009.

[65] C. G. J. McKenzie *et al.*, “Contribution of Candida albicans cell wall components to recognition by and escape from murine macrophages,” *Infect. Immun.*, vol. 78, no. 4, pp. 1650–1658, 2010.

[66] M. Wellington, K. Koselny, F. S. Sutterwala, and D. J. Krysan, “Candida albicans triggers NLRP3-mediated pyroptosis in macrophages,” *Eukaryot. Cell*, vol. 13, no. 2, pp. 329–340, 2014.

[67] N. Uwamahoro *et al.*, “The pathogen Candida albicans hijacks pyroptosis for escape from macrophages,” *MBio*, vol. 5, no. 2, pp. 1–11, 2014.

[68] L. Kasper *et al.*, “The fungal peptide toxin Candidalysin activates the NLRP3 inflammasome and causes cytolysis in mononuclear phagocytes,” *Nat. Commun.*, vol. 9, no. 1, 2018.

[69] J. M. Bain, L. E. Lewis, B. Okai, J. Quinn, N. A. R. Gow, and L. P. Erwig, “Non-lytic expulsion/exocytosis of Candida albicans from macrophages,” *Fungal Genet. Biol.*, vol. 49, no. 9, pp. 677–678, 2012.

[70] J. Schrenzel *et al.*, “Electron currents generated by the human phagocyte NADPH oxidase,” *Nature*, vol. 392, no. 6677, pp. 734–737, 1998.

[71] W. M. Nauseef, “The phagocyte NOX2 NADPH oxidase in microbial killing and cell signaling,” *Curr. Opin. Immunol.*, vol. 60, pp. 130–140, 2019.

[72] P. V. Seegren *et al.*, “Mitochondrial Ca2+ Signaling Is an Electrometabolic Switch to Fuel Phagosome Killing,” *Cell Rep.*, vol. 33, no. 8, p. 108411, 2020.

[73] L. M. Douglas and J. B. Konopka, “Plasma membrane architecture protects Candida albicans from killing by copper,” *PLoS Genet.*, vol. 15, no. 1, pp. 1–26, 2019.

[74] R. S. Flannagan, G. Cosío, and S. Grinstein, “Antimicrobial mechanisms of phagocytes and bacterial evasion strategies,” *Nat. Rev. Microbiol.*, vol. 7, no. 5, pp. 355–366, 2009.

[75] S. Vylkova, A. J. Carman, H. A. Danhof, J. R. Collette, H. Zhou, and M. C. Lorenz, “The fungal pathogen candida albicans autoinduces hyphal morphogenesis by raising extracellular pH,” *MBio*, vol. 2, no. 3, pp. 1–12, 2011.

[76] H. A. Danhof, S. Vylkova, E. M. Vesely, A. E. Ford, M. Gonzalez-Garay, and M.

C. Lorenz, “Robust extracellular pH modulation by Candida albicans during growth in carboxylic acids,” *MBio*, vol. 7, no. 6, 2016.

[77] S. Vylkova and M. C. Lorenz, “Modulation of Phagosomal pH by Candida albicans Promotes Hyphal Morphogenesis and Requires Stp2p, a Regulator of Amino Acid Transport,” *PLoS Pathog.*, vol. 10, no. 3, 2014.

[78] E. M. Vesely, R. B. Williams, J. B. Konopka, and M. C. Lorenz, “ N - Acetylglucosamine Metabolism Promotes Survival of Candida albicans in the Phagosome ,” *mSphere*, vol. 2, no. 5, 2017.

[79] S. Vylkova and M. C. Lorenz, “Phagosomal neutralization by the fungal pathogen Candida albicans induces macrophage pyroptosis,” *Infect. Immun.*, vol. 85, no. 2, 2017.

[80] H. A. Danhof and M. C. Lorenz, “The Candida albicans ATO gene family promotes neutralization of the macrophage phagolysosome,” *Infect. Immun.*, vol. 83, no. 11, pp. 4416–4426, 2015.

[81] J. Westman, G. Moran, S. Mogavero, B. Hube, and S. Grinstein, “Candida albicans Hyphal Expansion Causes Phagosomal Membrane Damage and Luminal Alkalinization,” *MBio*, vol. 9, no. 5, pp. 1–14, 2018.

[82] J. M. Bain *et al.*, “Immune cells fold and damage fungal hyphae,” *Proc. Natl. Acad. Sci. U. S. A.*, vol. 118, no. 15, pp. 1–8, 2021.

[83] J. Zimmerberg and M. M. Kozlov, “How proteins produce cellular membrane curvature,” *Nat. Rev. Mol. Cell Biol.*, vol. 7, no. 1, pp. 9–19, 2006.

[84] E. Evans, V. Heinrich, F. Ludwig, and W. Rawicz, “Dynamic tension spectroscopy and strength of biomembranes,” *Biophys. J.*, vol. 85, no. 4, pp. 2342–2350, 2003.

[85] J. Westman *et al.*, “Lysosome Fusion Maintains Phagosome Integrity during Fungal Infection,” *Cell Host Microbe*, pp. 1–15, 2020.

[86] A. Ballabio and J. S. Bonifacino, “Lysosomes as dynamic regulators of cell and organismal homeostasis,” *Nat. Rev. Mol. Cell Biol.*, vol. 21, no. 2, pp. 101–118, 2020.

[87] G. Parenti, G. Andria, and A. Ballabio, “Lysosomal storage diseases: From

pathophysiology to therapy," *Annu. Rev. Med.*, vol. 66, pp. 471–486, 2015.

[88] P. Saftig and J. Klumperman, "Lysosome biogenesis and lysosomal membrane proteins: Trafficking meets function," *Nat. Rev. Mol. Cell Biol.*, vol. 10, no. 9, pp. 623–635, 2009.

[89] J. Pu, C. M. Guardia, T. Keren-Kaplan, and J. S. Bonifacino, "Mechanisms and functions of lysosome positioning," *J. Cell Sci.*, vol. 129, no. 23, pp. 4329–4339, 2016.

[90] C. Papadopoulos, B. Kravic, and H. Meyer, "Repair or Lysophagy: Dealing with Damaged Lysosomes," *J. Mol. Biol.*, vol. 432, no. 1, pp. 231–239, 2020.

[91] F. Wang, R. Gómez-Sintes, and P. Boya, "Lysosomal membrane permeabilization and cell death," *Traffic*, vol. 19, no. 12, pp. 918–931, 2018.

[92] C. Papadopoulos and H. Meyer, "Detection and Clearance of Damaged Lysosomes by the Endo-Lysosomal Damage Response and Lysophagy," *Curr. Biol.*, vol. 27, no. 24, pp. R1330–R1341, 2017.

[93] I. Eriksson, P. Wäster, and K. Öllinger, "Restoration of lysosomal function after damage is accompanied by recycling of lysosomal membrane proteins," *Cell Death Dis.*, vol. 11, no. 5, 2020.

[94] L. M. Shaughnessy, A. D. Hoppe, K. A. Christensen, and J. A. Swanson, "Membrane perforations inhibit lysosome fusion by altering pH and calcium in Listeria monocytogenes vacuoles," *Cell. Microbiol.*, vol. 8, no. 5, pp. 781–792, 2006.

[95] M. L. Skowyra, P. H. Schlesinger, T. V. Naismith, and P. I. Hanson, "Triggered recruitment of ESCRT machinery promotes endolysosomal repair," *Science (80-.).*, vol. 360, no. 6384, 2018.

[96] D. J. Katzmann, M. Babst, and S. D. Emr, "Ubiquitin-dependent sorting into the multivesicular body pathway requires the function of a conserved endosomal protein sorting complex, ESCRT-I," *Cell*, vol. 106, no. 2, pp. 145–155, 2001.

[97] M. Babst, D. J. Katzmann, W. B. Snyder, B. Wendland, and S. D. Emr, "Endosome-associated complex, ESCRT-II, recruits transport machinery for protein sorting at the multivesicular body," *Dev. Cell*, vol. 3, no. 2, pp. 283–289,

2002.

[98] M. Babst, D. J. Katzmann, E. J. Estepa-Sabal, T. Meerloo, and S. D. Emr, “ESCRT-III: An endosome-associated heterooligomeric protein complex required for MVB sorting,” *Dev. Cell*, vol. 3, no. 2, pp. 271–282, 2002.

[99] M. Radulovic *et al.*, “ ESCRT -mediated lysosome repair precedes lysophagy and promotes cell survival ,” *EMBO J.*, vol. 37, no. 21, pp. 1–15, 2018.

[100] L. Christ, C. Raiborg, E. M. Wenzel, C. Campsteijn, and H. Stenmark, “Cellular Functions and Molecular Mechanisms of the ESCRT Membrane-Scission Machinery,” *Trends Biochem. Sci.*, vol. 42, no. 1, pp. 42–56, 2017.

[101] L. Christ, E. M. Wenzel, K. Liestøl, C. Raiborg, C. Campsteijn, and H. Stenmark, “ALIX and ESCRT-I/II function as parallel ESC RT-III recruiters in cytokinetic abscission,” *J. Cell Biol.*, vol. 212, no. 5, pp. 499–513, 2016.

[102] J. Jia *et al.*, “Galectin-3 Coordinates a Cellular System for Lysosomal Repair and Removal,” *Dev. Cell*, vol. 52, no. 1, pp. 69-87.e8, 2020.

[103] E. Mittal *et al.*, “Mycobacterium tuberculosis type VII secretion system effectors differentially impact the ESCRT endomembrane damage response,” *MBio*, vol. 9, no. 6, pp. 1–21, 2018.

[104] S. Herbst *et al.*, “ LRRK 2 activation controls the repair of damaged endomembranes in macrophages ,” *EMBO J.*, vol. 39, no. 18, pp. 1–14, 2020.

[105] M. Radulovic and H. Stenmark, “ LRRK 2 to the rescue of damaged endomembranes ,” *EMBO J.*, vol. 39, no. 18, pp. 2–4, 2020.

[106] J. Westman *et al.*, “Calcium-Dependent ESCRT Recruitment and Lysosome Exocytosis Maintain Epithelial Integrity During Candida albicans Invasion,” *Cell Host Microbe*, p. 50, 2021.

[107] U. Repnik *et al.*, “L-leucyl-L-leucine methyl ester does not release cysteine cathepsins to the cytosol but inactivates them in transiently permeabilized lysosomes,” *J. Cell Sci.*, vol. 130, no. 18, pp. 3124–3140, 2017.

[108] C. F. Daussy and H. Wodrich, “‘Repair Me if You Can’: Membrane Damage, Response, and Control from the Viral Perspective,” 2020.

[109] L. Koerver *et al.*, " The ubiquitin-conjugating enzyme UBE 2 QL 1 coordinates lysophagy in response to endolysosomal damage ," *EMBO Rep.*, vol. 20, no. 10, pp. 1–17, 2019.

[110] C. S. Peskin *et al.*, "A Gene Network Regulating Lysosomal Biogenesis and Function," *Science (80-.).*, no. July, pp. 473–478, 2009.

[111] D. L. Medina *et al.*, "Lysosomal calcium signalling regulates autophagy through calcineurin and TFEB," *Nat. Cell Biol.*, vol. 17, no. 3, pp. 288–299, 2015.

[112] A. Roczniak-Ferguson *et al.*, "The Transcription Factor TFEB Links mTORC1 Signaling to Transcriptional Control of Lysosome Homeostasis," *Sci. Signal.*, 2012.

[113] F. Hofmann *et al.*, "Cx43-gap junctions accumulate at the cytotoxic immunological synapse enabling cytotoxic T lymphocyte melanoma cell killing," *Int. J. Mol. Sci.*, vol. 20, no. 18, pp. 1–16, 2019.

[114] Y. Huang *et al.*, "Connexin43 is required for the effective activation of spleen cells and immunoglobulin production," *Int. J. Mol. Sci.*, vol. 20, no. 22, pp. 1–15, 2019.

[115] L. Medina-Ceja, J. C. Salazar-Sánchez, J. Ortega-Ibarra, and A. Morales-Villagrán, "Connexins-based hemichannels/channels and their relationship with inflammation, seizures and epilepsy," *Int. J. Mol. Sci.*, vol. 20, no. 23, pp. 1–17, 2019.

[116] T. Martins-Marques, T. Ribeiro-Rodrigues, D. Batista-Almeida, T. Aasen, B. R. Kwak, and H. Girao, "Biological Functions of Connexin43 Beyond Intercellular Communication," *Trends Cell Biol.*, vol. 29, no. 10, pp. 835–847, 2019.

[117] T. Aasen, M. Mesnil, C. C. Naus, P. D. Lampe, and D. W. Laird, "Gap junctions and cancer: Communicating for 50 years," *Nat. Rev. Cancer*, vol. 16, no. 12, pp. 775–788, 2016.

[118] D. W. Laird, "Life cycle of connexins in health and disease," *Biochem. J.*, vol. 394, no. 3, pp. 527–543, 2006.

[119] T. M. Ribeiro-Rodrigues, T. Martins-Marques, S. Morel, B. R. Kwak, and H. Girão, "Role of connexin 43 in different forms of intercellular communication –

gap junctions, extracellular vesicles and tunnelling nanotubes," *J. Cell Sci.*, vol. 130, no. 21, pp. 3619–3630, 2017.

[120] J. L. Esseltine and D. W. Laird, "Next-Generation Connexin and Pannexin Cell Biology," *Trends Cell Biol.*, vol. 26, no. 12, pp. 944–955, 2016.

[121] D. W. Laird and P. D. Lampe, "Therapeutic strategies targeting connexins," *Nat. Rev. Drug Discov.*, vol. 17, no. 12, pp. 905–921, 2018.

[122] E. Leithe, M. Mesnil, and T. Aasen, "The connexin 43 C-terminus: A tail of many tales," *Biochim. Biophys. Acta - Biomembr.*, vol. 1860, no. 1, pp. 48–64, 2018.

[123] M. S. C. Fontes, T. A. B. Van Veen, J. M. T. De Bakker, and H. V. M. Van Rijen, "Functional consequences of abnormal Cx43 expression in the heart," *Biochim. Biophys. Acta - Biomembr.*, vol. 1818, no. 8, pp. 2020–2029, 2012.

[124] T. Martins-Marques *et al.*, "Ischaemia-induced autophagy leads to degradation of gap junction protein connexin43 in cardiomyocytes," *Biochem. J.*, vol. 467, no. 2, pp. 231–245, 2015.

[125] T. M. Ribeiro-Rodrigues *et al.*, "AMSH-mediated deubiquitination of Cx43 regulates internalization and degradation of gap junctions," *FASEB J.*, vol. 28, no. 11, pp. 4629–4641, 2014.

[126] E. Bejarano *et al.*, "Autophagy modulates dynamics of connexins at the plasma membrane in a ubiquitin-dependent manner," *Mol. Biol. Cell*, vol. 23, no. 11, pp. 2156–2169, 2012.

[127] A. R. Soares *et al.*, "Gap junctional protein Cx43 is involved in the communication between extracellular vesicles and mammalian cells," *Sci. Rep.*, vol. 5, no. January, pp. 1–14, 2015.

[128] D. Batista-Almeida *et al.*, "Ischaemia impacts TNT-mediated communication between cardiac cells," *Curr. Res. Cell Biol.*, vol. 1, no. January, p. 100001, 2020.

[129] A. M. Glass, E. G. Snyder, and S. M. Taffet, "Connexins and pannexins in the immune system and lymphatic organs," *Cell. Mol. Life Sci.*, vol. 72, no. 15, pp. 2899–2910, 2015.

[130] F. Rinaldi *et al.*, "Cross-regulation of Connexin43 and β-catenin influences

differentiation of human neural progenitor cells.," *Cell Death Dis.*, vol. 5, pp. 1–9, 2014.

[131] J. Ariazi *et al.*, "Tunneling nanotubes and gap junctions–their role in long-range intercellular communication during development, health, and disease conditions," *Front. Mol. Neurosci.*, vol. 10, no. October, pp. 1–12, 2017.

[132] W. Li *et al.*, "Connexin 43 Hemichannel as a Novel Mediator of Sterile and Infectious Inflammatory Diseases," *Sci. Rep.*, vol. 8, no. 1, pp. 1–15, 2018.

[133] C. Y. Xu, W. S. Zhang, H. Zhang, Y. Cao, and H. Y. Zhou, "The Role of Connexin-43 in the Inflammatory Process: A New Potential Therapy to Influence Keratitis," *J. Ophthalmol.*, vol. 2019, no. Figure 1, 2019.

[134] S. Morel *et al.*, "Titration of the gap junction protein Connexin43 reduces atherogenesis," *Thromb. Haemost.*, vol. 112, no. 2, pp. 390–401, 2014.

[135] R. D. Cheng, J. J. Ren, Y. Y. Zhang, and X. M. Ye, "P2X4 receptors expressed on microglial cells in post-ischemic inflammation of brain ischemic injury," *Neurochem. Int.*, vol. 67, no. 1, pp. 9–13, 2014.

[136] M. A. Retamal *et al.*, "Cx43 hemichannels and gap junction channels in astrocytes are regulated oppositely by proinflammatory cytokines released from activated microglia," *J. Neurosci.*, vol. 27, no. 50, pp. 13781–13792, 2007.

[137] S. Chauhan *et al.*, "TRIMs and Galectins Globally Cooperate and TRIM16 and Galectin-3 Co-direct Autophagy in Endomembrane Damage Homeostasis," *Dev. Cell*, vol. 39, no. 1, pp. 13–27, 2016.

[138] T. M. Ribeiro-Rodrigues *et al.*, "Exosomes secreted by cardiomyocytes subjected to ischaemia promote cardiac angiogenesis," *Cardiovasc. Res.*, vol. 113, no. 11, pp. 1338–1350, 2017.

[139] W. A. Basheer *et al.*, "GJA1-20k Arranges Actin to Guide Cx43 Delivery to Cardiac Intercalated Discs," pp. 1069–1080, 2017.

[140] Y. Zhen, M. Radulovic, M. Vietri, and H. Stenmark, "Sealing holes in cellular membranes," *EMBO J.*, vol. 40, no. 7, pp. 1–13, 2021.

[141] A. J. Jimenez, P. Maiuri, J. Lafaurie-Janvore, S. Divoux, M. Piel, and F. Perez, "ESCRT machinery is required for plasma membrane repair," *Science (80-.).*,

vol. 343, no. 6174, 2014.

[142] L. L. Scheffer *et al.*, “Mechanism of Ca^{2+}-triggered ESCRT assembly and regulation of cell membrane repair,” *Nat. Commun.*, vol. 5, p. 5646, 2014.

[143] J. Robijns, G. Houthaeve, K. Braeckmans, and W. H. De Vos, “Loss of Nuclear Envelope Integrity in Aging and Disease,” *Int. Rev. Cell Mol. Biol.*, vol. 336, pp. 205–222, 2018.

[144] L. Penfield *et al.*, “Dynein pulling forces counteract lamin-mediated nuclear stability during nuclear envelope repair,” *Mol. Biol. Cell*, vol. 29, no. 7, pp. 852–868, 2018.

[145] M. Raab *et al.*, “ESCRT III repairs nuclear envelope ruptures during cell migration to limit DNA damage and cell death,” *Science (80-.).*, vol. 352, no. 6283, pp. 359–362, 2016.

[146] C. M. Denais *et al.*, “Nuclear envelope rupture and repair during cancer cell migration,” *Science (80-.).*, vol. 352, no. 6283, pp. 353–358, 2016.

[147] A. T. López-Jiménez *et al.*, “The ESCRT and autophagy machineries cooperate to repair ESX-1-dependent damage at the Mycobacterium-containing vacuole but have opposite impact on containing the infection,” *PLoS Pathog.*, vol. 14, no. 12, pp. 1–29, 2018.

[148] I. D. Jacobsen *et al.*, “Candida albicans dimorphism as a therapeutic target,” vol. 7210, 2014.

[149] L. C. Gomes and I. Dikic, “Autophagy in antimicrobial immunity,” *Mol. Cell*, vol. 54, no. 2, pp. 224–233, 2014.

[150] M. Di Rienzo, A. Romagnoli, M. Antonioli, M. Piacentini, and G. M. Fimia, “TRIM proteins in autophagy: selective sensors in cell damage and innate immune responses,” *Cell Death Differ.*, vol. 27, no. 3, pp. 887–902, 2020.

[151] T. Kimura *et al.*, “ Dedicated SNARE s and specialized TRIM cargo receptors mediate secretory autophagy ,” *EMBO J.*, vol. 36, no. 1, pp. 42–60, 2017.

[152] M. S. Gibson, N. Domingues, and O. V. Vieira, “Lipid and non-lipid factors affecting macrophage dysfunction and inflammation in atherosclerosis,” *Front. Physiol.*, vol. 9, no. JUN, 2018.

[153] K. Schroder and J. Tschopp, “The Inflammasomes,” *Cell*, vol. 140, no. 6, pp. 821–832, 2010.

[154] M. Ito *et al.*, “Bruton’s tyrosine kinase is essential for NLRP3 inflammasome activation and contributes to ischaemic brain injury,” *Nat. Commun.*, vol. 6, 2015.

[155] T. R. O’meara *et al.*, “High-throughput screening identifies genes required for Candida albicans induction of macrophage pyroptosis,” *MBio*, vol. 9, no. 4, 2018.

[156] O. Gross *et al.*, “Syk kinase signalling couples to the Nlrp3 inflammasome for anti-fungal host defence,” *Nature*, vol. 459, no. 7245, pp. 433–436, 2009.

[157] A. G. Hise *et al.*, “An Essential Role for the NLRP3 Inflammasome in Host Defense against the Human Fungal Pathogen Candida albicans,” *Cell Host Microbe*, vol. 5, no. 5, pp. 487–497, 2009.

[158] O. Rogiers *et al.*, “Candidalysin Crucially Contributes to Nlrp3 Inflammasome Activation by Candida albicans Hyphae,” *MBio*, vol. 10, no. 1, 2019.

[159] M. Fraiberg and Z. Elazar, “A TRIM16-Galactin3 Complex Mediates Autophagy of Damaged Endomembranes,” *Dev. Cell*, vol. 39, no. 1, pp. 1–2, 2016.

[160] K. M. Brothers, R. L. Gratacap, S. E. Barker, Z. R. Newman, A. Norum, and R. T. Wheeler, “NADPH Oxidase-Driven Phagocyte Recruitment Controls Candida albicans Filamentous Growth and Prevents Mortality,” *PLoS Pathog.*, vol. 9, no. 10, 2013.

[161] J. M. Tam *et al.*, “Dectin-1-dependent LC3 recruitment to phagosomes enhances fungicidal activity in macrophages,” *J. Infect. Dis.*, vol. 210, no. 11, pp. 1844–1854, 2014.

[162] M. Kanayama, M. Inoue, K. Danzaki, G. Hammer, Y. W. He, and M. L. Shinohara, “Autophagy enhances NFκB activity in specific tissue macrophages by sequestering A20 to boost antifungal immunity,” *Nat. Commun.*, vol. 6, pp. 1–14, 2015.

[163] D. W. Laird, K. L. Puranam, and J. P. Revel, “Turnover and phosphorylation dynamics of connexin43 gap junction protein in cultured cardiac myocytes,” *Biochem. J.*, vol. 273, no. 1, pp. 67–72, 1991.

[164] M. A. Beardslee, J. G. Laing, E. C. Beyer, and J. E. Saffitz, “Rapid turnover of

connexin43 in the adult rat heart," *Circ. Res.*, vol. 83, no. 6, pp. 629–635, 1998.

[165] H. Qin, Q. Shao, S. A. Igdoura, M. A. Alaoui-Jamali, and D. W. Laird, "Lysosomal and proteasomal degradation play distinct roles in the life cycle of Cx43 in gap junctional intercellular communication-deficient and -competent breast tumor cells," *J. Biol. Chem.*, vol. 278, no. 32, pp. 30005–30014, 2003.

[166] C. Ambrosi *et al.*, "Connexin43 forms supramolecular complexes through non-overlapping binding sites for drebrin, tubulin, and ZO-1," *PLoS One*, vol. 11, no. 6, pp. 1–23, 2016.

[167] R. E. Strauss and R. G. Gourdie, "Cx43 and the actin cytoskeleton: Novel roles and implications for cell-cell junction-based barrier function regulation," *Biomolecules*, vol. 10, no. 12, pp. 1–27, 2020.

[168] A. N. Atre, S. V. Surve, Y. S. Shouche, J. Joseph, M. S. Patole, and R. L. Deopurkar, "Association of small Rho GTPases and actin ring formation in epithelial cells during the invasion by Candida albicans," *FEMS Immunol. Med. Microbiol.*, vol. 55, no. 1, pp. 74–84, 2009.

[169] L. E. Wicki-stordeur and L. A. Swayne, "Panx1 regulates neural stem and progenitor cell behaviours associated with cytoskeletal dynamics and interacts with multiple cytoskeletal elements," no. Dcx, pp. 1–8, 2013.